Regd. No. C-3911

VOL. 34 **INDIAN JOURNAL OF PHYSICS** No. 8

(Published in collaboration with the Indian Physical Society)

AND

VOL. 43 **PROCEEDINGS** No. 8

OF THE

INDIAN ASSOCIATION FOR THE CULTIVATION OF SCIENCE

AUGUST 1960

PUBLISHED BY THE
INDIAN ASSOCIATION FOR THE CULTIVATION OF SCIENCE
JADAVPUR, CALCUTTA 32

Annual Subscription—
Inland Rs. 25.00
Foreign £ 2-10-0 or $ 7.00

NOTICE TO INTENDING AUTHORS

Manuscripts for publication should be sent to the Assistant Editor, Indian Journal of Physics, Jadavpur, Calcutta-32.

The manuscripts submitted must be type-written with double space on thick foolscap paper with sufficient margin on the left and at the top. The original copy, and not the carbon copy, should be submitted. Each paper must contain an Abstract at the beginning.

All References should be given in the text by quoting the surname of the author, followed by year of publication, *e.g.*, (Roy, 1958). The full Reference should be given in a list at the end, arranged alphabatically, as follows; Roy, S. B., 1958, *Ind. J. Phys.*, **32,** 323.

Line diagrams should be drawn on white Bristol board or tracing paper with black Indian ink, and letters and numbers inside the diagrams should be written neatly in capital type with Indian ink. The size of the diagrams submitted and the lettering inside should be large enough so that it is legible after reduction to one-third the original size. A simple style of lettering such as gothic, with its uniform line width and no serifs should be used, *e.g.*,

A·B·E·F·G·M·P·T·W·

Photographs submitted for publication should be printed on glossy paper with somewhat more contrast than that desired in the reproduction, and should, if possible be mounted on thick white paper.

Captions to all figures should be typed in a separate sheet and attached at the end of the paper.

The mathematical expressions should be written carefully by hand. Care should be taken to distinguish between capital and small letters and superscripts and subscripts. Repetition of a complex expression should be avoid by representing it by a symbol. Greek letters and unusual symbols should be identified in the margin. Fractional exponents should be used instead of root signs.

NUCLEAR SPIN ECHOES AND MOLECULAR SELF-DIFFUSION IN LIQUIDS

S. K. GHOSH AND S. K. SINHA

SAHA INSTITUTE OF NUCLEAR PHYSICS, CALCUTTA

(*Received July* 8, 1960)

ABSTRACT. The nuclear spin-echo phenomenon and the effect of molecular self-diffusion in liquids on the spin-echoes have been treated on the basis of a new stochastic model. The physical and mathematical inconsistencies of similar treatments reported earlier have also been discussed. A spin-echo method for measuring the co-efficient of molecular self-diffusion D directly, using the "image echo" has been developed, which completely eliminates the relaxation damping of the echo signal. It has also been shown that the diffusion damping co-efficient k thus determined can be utilized for an independent measurement of transverse relaxation time T_2 even in presence of appreciable diffusion. These methods have been used in the case of water, and the values of D and T_2 obtained agree well with other measurements. Further, a direct experimental check has been furnished to compare the validity of different theoretical approaches to this problem.

I. INTRODUCTION

The mechanism of formation of nuclear spin-echoes and the effect of molecular self-diffusion on the echo-amplitudes have been discussed previously by various authors [Hahn (1950), Das and Saha (1954), Carr and Purcell (1954), Herzog and Hahn (1956), Torrey (1956) and Douglass and McCall (1958)]. The equilibrium (thermal) magnetization of a substance when placed in a steady magnetic field, is deflected from the direction of the magnetic field by a short radio frequency (*rf*) pulse and during the absence of the pulse the nuclear magnets execute Larmor precession (*Lp*) about the steady field with different Larmor frequencies (*Lf*) because of inhomogeneity in the magnetic field. After a certain time-interval τ, if a second short *rf* pulse is used to reverse the phase accumulated by the nuclear magnets, the nuclei will recluster completely at the end of the next interval τ and give the echo signal. This complete reclustering will be possible only when the phase accumulations of individual groups are equal in the two intervals. If, however, there be any process that makes these phase accumulations unequal, the reclustering at the end of the interval 2τ will not be complete and the echo amplitude will diminish. The diminution will depend on τ if the phase accumu-

* One should note that the random motion of the molecules will also average out the "local field" and give rise to relaxation damping of the nuclear induction signals. T_1 and T_2 in Bloch equations (1) take account of this effect.

lation due to that process is time dependent. The random (Brownian) motion of the molecules in a liquid is such a process*. This process carries the molecules along with the resonating nuclei to different sites in the inhomogeneous magnetic field, thereby changing their Lf and hence the phase of their Lp. Since this is a Markoffian process, the phase-accumulations will not be proportional to first power of time, and as a result they will not be equal in the two intervals. Thus, there will be damping of the echo-amplitude which has been called the diffusion damping by Hahn. If instead of two pulses, three pulses are used to form the echoes the above effect of molecular self-diffusion will manifest itself in the different echoes in different ways. This effect has been discussed by Hahn and later corrected by Herzog and Hahn and by Das and Saha in the three-pulse echo system. Their methods have been examined in some details at the end of Section II.

The present work considers the following model. The random molecular motion is described by the motion of any representative molecule with proper initial distribution in Larmor frequencies (conforming with the actual physical situation). Such a distribution can be represented by Dirac's δ-function as in the case of liquid molecules executing Brownian motion [Green (1952)]. The whole time-interval in which we are interested is divided into a large number of small sub-intervals, and the damping of the echo signal due to random phase-accumulations in the successive short intervals, that arise through random change in Larmor frequency has been taken into account through the change in Larmor frequency which follows a Markoff process* [Chandrashekhar (1943), Wang and Uhlenbeck (1945), Anderson (1954), Herzog and Hahn (1956)], satisfying Chapman-Kolmogoroff equation. The results of such calculation agree with those from the straightforward treatments of Carr and Purcell and of Torrey when extended to echoes for Carr-Purcell pulse sequence.

On the basis of this formulation, experimental methods for the determination of self-diffusion constant, D, and the transverse relaxation time T_2, have been developed. In these methods the diffusion-damping co-efficient k ($= \gamma^2 G^2 D$, where γ, G and D have the usual meaning) can be obtained without previous determination of T_2. This value of k is then used to obtain T_2 from Carr-Purcell method in general cases, which has been described in details in Section IV. Besides obtaining a satisfactory value for D and T_2, an independent experimental check of the physical basis of the theoretical formulation has also been described.

In Section II, the theoretical formulation is presented with criticism of Das and Saha's and of Herzog and Hahn's treatments. In Section III, the apparatus used is briefly described. The Section IV contains the experimental methods for

---

* A collection of the relevant papers on Markoff Process can be found in "Noise and Stochastic Processes", edited by N. Wax., Dover Publications, New York, (1954).

measurement of D and T_2, and the results. In the last Section V, the different experimental methods for measuring D and T_2 have been critically examined.

II. THEORETICAL FORMULATION

Let us start with the Bloch equations (Bloch, 1946) which have been proved satisfactory in describing the dynamical behaviour of nuclear magnetization. The equations can be written in a co-ordinate system rotating with the pulsed-*rf* frequency, ω as [Bloch, 1946; Rabi *et al.*, 1954].

$$\frac{du}{dt} + \eta v = -\frac{u}{T_2}$$

$$\frac{dv}{dt} - \eta u + Rw = -\frac{v}{T_2}$$

and

$$\frac{dw}{dt} - Rv = -\frac{w-w_0}{T_1} \qquad \ldots \quad (1)$$

Here u, v, w, w_0 and η have a slightly different meaning than the usual. The molecules carrying the nuclear magnets execute random (Brownian) motion in an externally applied inhomogeneous magnetic field. To take account of the effect of this random motion on the spin-echo phenomenon, the Bloch equations have been assumed to be true for the average magnetization of a molecule at a point (x, y, z) inside the sample. u, v and w are the x', y' and z' components, respectively of the average molecular magnetization $\boldsymbol{M}_{mol}$. w_0 is the equilibrium value of magnetization at thermal equilibrium and is given by $w_0 = \chi_{mol}\, H_z\, (x,\ y,\ z)$, χ_{mol} being the static molecular susceptibility, $R = \gamma H_1$ and $\eta = \gamma H_z\,(x, y, z) - \omega$; H_1 is the half amplitude of the applied linearly polarised *rf* field, $2H_1 \cos \omega t$.

One of the two circularly polarized components of the *rf* field is actually effective in producing resonance. $H_z\ (x, y, z)$ is the value of the externally applied magnetic field at the point (x, y, z). T_1 and T_2 are the usual longitudinal and transverse relaxation times respectively as introduced by Bloch. The random change of position of the molecule causes a corresponding change in the value of η. This random motion is of the nature of the stationary Markoff process. On the average this motion is well represented by the Langevin equation (Kirkwood, 1946 & Green, 1952).

In order to find out the magnetization under study at any subsequent time from its initial value we have to follow the motion of such a molecule. In following the motion of the molecule we shall have to keep in mind that the magnetization must satisfy the Bloch equations whereas its position co-ordinates and hence η will be obtaind from the Langevin equation. For the solution of the

Bloch equations under such conditions we divide the whole time interval from the start of the pulse sequence into a large number of small sub-intervals. These sub-intervals are of such magnitude that the root mean square change in η is very small. Under such conditions we can solve the Bloch equations during these sub-intervals taking η to be constant; the stochastic nature of η is taken into account through the inclusion of a transition probability corresponding to the change in η from its initial value at the beginning of the sub-interval to the final value at the end of the sub-interval. The integration over the initial value of η for the interval will give us the value of magnetization at the time we are interested in, and it is a function of η corresponding to that time.

Analytically, let $\Phi(\eta_s, t_s)$ be the solution of the Bloch equations for a certain value of $\eta(=\eta_s)$. Since η is a stochastic variable, the value of magnetization with a certain value of $\eta(=\eta_s)$ must be expressed as

$$F[\eta_s, t_s] = \Phi(\eta_s, t_s) W(\eta_s, t_s)$$

where $W(\eta_s, t_s)$ expresses the probability that at time t_s we have the value of η as η_s. As η follows a Markoff process $F[\eta_s, t_s]$ can be related with its value at any other time by a relation like the Chapman-Kolmogoroff equation :

$$F[\eta_s, t_s] = \int_{-\infty}^{\infty} F[\eta_i, t_i]\ T(\eta_s, t_s \,|\, \eta_i, t_i)\ d\eta_i$$

Here $T(\eta_s, t_s/\eta_i, t_i)$ denotes the transition probability of the change of η_i to η_s in time $t_s - t_i$. This transition probability, in general, will be product of two transition probabilities, namely $B(\eta_s, t_s/\eta_i, t_i)$ and $P(\eta_s, t_s/\eta_i, t_i)$. The first one is obtainable from the solution of Bloch equations if we could treat η also to be varying during the period. The second one can be obtained from the solution of Langevin equation. Now, if the time-interval $t_s - t_i$ is considered to be very small such that the change in η during the interval is small, but is of sufficient magnitude such that the force causing the displacements of the particles and hence the change of η fluctuates a large number of times, we have

$$B(\eta_s, t_s \,|\, \eta_i, t_i) \simeq B(\eta_i, t_s \,|\, \eta_i, t_i)$$

and $$P(\eta_s, t_s | \eta_i, t_i) \simeq \left\{ \frac{1}{4\pi k(t_s - t_i)} \right\}^{\frac{1}{2}} \exp \left\{ - \frac{(\eta_s - \eta_i)^2}{4k(t_s - t_i)} \right\}$$

(see expression (6))

with these assumptions,

$$F[\eta_s, t_s] = \int_{-\infty}^{\infty} \Phi(\eta_i, t_i) B(\eta_i, t_s \,|\, \eta_i, t_i)\ W(\eta_i, t_i)\ P(\eta_s, t_s \,|\, \eta_i, t_i) d\eta_i$$

$$= \int_{-\infty}^{\infty} \Phi(\eta_i, t_s) W(\eta_i, t_i)\ P(\eta_s, t_s \,|\, \eta_i, t_i) d\eta_i$$

This relation shows that if we know the initial value of F, we can deduce its value at any other time.

Let us now consider a particle situated initially at the point (x_0, y_0, z_0). The magnetization at $t = 0$ can be represented by

$$u[0, \eta] = u(0)W(\eta, 0) = 0$$

$$v[0, \eta] = v(0)W(\eta, 0) = 0$$

and

$$\omega[0, \eta] = w(0)W(\eta, 0) = w_0\delta(\eta - \eta_0) \qquad \ldots \quad (2)$$

The initial distribution has been taken in the form of Dirac δ-function as the position of the particle is definite at the point (x_0, y_0, z_0), and hence $\eta_0 = \gamma H_z(x_0, y_0, z_0) - \omega$. For the most general field distribution

$$H_z(x_0, y_0, z_0) = H_z(0) + x_0\left(\frac{dH_z}{dx}\right)_0 + y_0\left(\frac{dH_z}{dy}\right)_0 + z_0\left(\frac{dH_z}{dz}\right)_0 + \ldots$$

terms with higher derivatives of H_z. $H_z(0)$ is the value of the steady magnetic field at the origin. For simplicity the field gradient can be taken to be constant and unidirectional (in the direction of z), and η_0 can be written as

$$\eta_0 = \gamma H_z(0) - \omega + \gamma G z_0 \qquad \ldots \quad (3)$$

where $G = \dfrac{dH_z}{dz}$. At exact resonance $\gamma H_z(0) - \omega = 0$. The treatment, which has been followed here for this simple case, can be easily shown to be valid for multi-directional field gradients as well as for off-resonance conditions*.

Hence, considering any time-interval t, we divide it into a large number, say n of small and equal sub-intervals of Δt each, such that $n\Delta t = t$ and assign values to η at the beginning and at the end of each sub-interval. For example, η_{m-1} and η_m are these values for the m-th sub-interval. For the m-th sub-interval the Bloch equations are solved taking η_{m-1} to be constant, and we obtain $\phi(\eta_{m-1},$

* Since the results of this formulation (taking the field gradient in the z-direction as constant, and neglecting the field gradients in other directions) are used to interpret data obtained with a magnet where these conditions are not strictly valid, it is interesting to investigate the effects due to (a) G being not constant, and (b) the gradients in the x and y directions are not zero. It can be easily shown that none of these affects the result appreciably. Both the situations, described above, introduce small error in the value of k, but the time-dependence of the signal amplitudes remains almost unaffected. To test these points experimentally, the time dependence of the amplitude of the image echo was recorded without applying any field gradient in z-direction externally. Even in this case (where the field-gradient is multidirectional) the time dependence was found to be parabolic as the equation (14) predicts.

$m\Delta t$) where ϕ stands for u, v and w components. $F[\eta_m, m\Delta t]$ is then obtained by using the relation

$$F[\eta_m, m\Delta t] = \int_{-\infty}^{\infty} F[\eta_{m-1}, m\Delta t]\, P(\eta_m, \Delta t \,|\, \eta_{m-1}) d\eta_{m-1} \quad \ldots \quad (4)$$

where $P(\eta_m, \Delta t \,|\, \eta_{m-1})$ is the probability of η_{m-1} changing to η_m in the time-interval Δt. Using the relation

$$\eta_m - \eta_{m-1} = \gamma G(z_m - z_{m-1}) \quad \ldots \quad (5)$$

$P(\eta_m, \Delta t\ \eta_{m-1})$ can be obtained from the solution of Langevin equations, and the expression for it comes out as

$$P(\eta_m, \Delta t \,|\, \eta_{m-1}) = \left(\frac{1}{4\pi k \Delta t} \right)^{\frac{1}{2}} \exp \left\{ -\frac{(\eta_m - \eta_{m-1})^2}{4k\Delta t} \right\} \quad \ldots \quad (6)$$

where $k = \gamma^2 G^2 D$, D being the co-efficient of molecular self-diffusion. The Eq. (1) take different forms in the presence and in the absence of the *rf*-pulse, and the usual solutions in the two cases are each treated as ϕ as discussed above. The thermal equilibrium value of w-component can be shown to be given by

$$w_0[\eta_n, n\Delta t] = w_0 \int_{-\infty}^{\infty} \delta(\eta - \eta_0)\, P(\eta_n, n\Delta t \,|\, \eta) d\eta = w_0\, P(\eta_n, n\Delta t \,|\, \eta_0) \quad \ldots \quad (7)$$

The final value of $F(t)$ is then obtained from the relation

$$F(t) = \int_{-\infty}^{\infty} F[\eta_n, n\Delta t] d\eta_n \quad \ldots \quad (8)$$

This is the value of magnetization for a single particle. We obtain the total magnetization $M(t)$ due to the whole sample by using the relation

$$M(t) = N \iiint F(t) dV \quad \ldots \quad (9)$$

where the integration extends over the whole sample volume and N is the number density of the molecules.

For a cylindrical sample-holder and for the constant field gradient in the z-direction, the volume integral gives an expression of the form

$$\frac{2M_0 J_1(p)}{p} \quad \ldots \quad (10)$$

where for primary echo,

$$p = \gamma G a(t - 2\tau_1) \quad \ldots \quad (11)$$

Expressions for the echoes and the free induction signals for three pulses of nutational angles ξ_1, ξ_2 and ξ_3, applied at times $t = 0$, τ_1 and τ_2 respectively, as obtained by the present treatment.

Position of the signals	Time independent part of the amplitudes at signal maxima	Time dependent part of the amplitudes at the signal maxima	
		Part dependent on relaxation	Part dependent on molecular self diffusion
0	$-M_0 \sin \xi_1$	1	1
τ_1	$-M \sin \xi_2$	$1+(\cos \xi_1-1) \exp\left(-\frac{\tau_1}{T_1}\right)$	1
τ_2	$-M_0 \sin \xi_3$	$1+\left[\left\{1+(\cos \xi_1-1) \exp\left(-\frac{\tau_1}{T_1}\right)\right\} \times \cos \xi_2-1\right] \exp\left(-\frac{\tau_2-\tau_1}{T_1}\right)$	1
$2\tau_1$	$M_0 \sin \xi_1 \sin^2 (\xi_2/2)$	$\exp\left(-\frac{2\tau_1}{T_2}\right)$	$\left[\exp\left(-\frac{2}{3} k \tau_1^3\right)\right]$
$2\tau_2$	$M_0 \sin \xi_1 \cos^2 (\xi_2/2) \sin^2 (\xi_3/2)$	$\exp\left(-\frac{2\tau_2}{T_2}\right)$	$\left[\exp\left(-\frac{2}{3} k \tau_2^3\right)\right]$
$2(\tau_2-\tau_1)$ (Image echo)	$-M_0 \sin \xi_1 \sin^2 (\xi_2/2) \sin^2 (\xi_3/2)$	$\exp\left[-\frac{2(\tau_2-\tau_1)}{T_2}\right]$	$\left[\exp\left[-\frac{2}{3}\left\{k\tau_1^3+(\tau_2-2\tau_1)^3\right\}\right]\right]$
$[2\tau_2-\tau_1]$	$[M_0 \sin \xi_2 \sin^2 (\xi_3/2)]$	$\left[1+(\cos \xi_1-1) \exp\left(-\frac{\tau_1}{T_1}\right)\right] \times \exp\left[-\frac{2(\tau_1-\tau_1)}{T_2}\right]$	$\exp\left[-\frac{2}{3} k(\tau_2-\tau_1)^3\right]$
$\tau_2+\tau_1$	$\frac{1}{2} M_0 \sin \xi_1 \sin \xi_2 \sin \xi_3$	$\exp\left[-\frac{2\tau_1}{T_2}-\frac{\tau_2-\tau_2}{T_1}\right]$	$\exp\left[-k\left\{\frac{2}{3}\tau_1^3+\tau_1^2(\tau_2-\tau_1)\right\}\right]$
$2n\tau$ (Carr-Parcell echoes*)	$(-1)^{n-1} M_0$	$\exp\left[-\frac{2n\tau}{T_2}\right]$	$\exp\left[-\frac{2}{3} kn\tau_3\right]$

* Echoes obtained at time $t=2n$ after the application of a series of n 180° pulses at times $t=(2n-1)$ following a 90° pulse applied at $t=0$.

a is the internal radius of the sample holder, J_1 is the first order Bessel function of the first kind. This represents the shape of the echo and of the free induction signals. For constant field gradients in the three directions, this is given by

$$\frac{2M_0 J_1(p)}{p} \cdot \frac{\sin q}{q} \qquad \ldots \quad (12)$$

where for primary echo,

$$p = \gamma \left\{ \left(\frac{dH_z}{dz}\right)^2 + \left(\frac{dH_z}{dx}\right)^2 \right\}^{\frac{1}{2}} a(t-2\tau_1)$$

and

$$q = \gamma \left(\frac{dH_z}{dy}\right) b(t-2\tau_1) \qquad \ldots \quad (13)$$

b is the effective length of the sample.

Using the above scheme and the usual technique of matching the Bloch equations, the different free induction signals and the different echo signals for any number of pulses of arbitrary nutational angles can be obtained. The results of such calculations for three pulses applied at time $t = 0$, τ_1 and τ_2 are shown in Table I. Table I also contains the expressions for the amplitudes of the echoes occurring at $t = 2n\tau_1$, when a first 90°-pulse followed by a series of n 180°-pulses are applied at times $t = \tau_1, 3\tau_1, \ldots (2n-1)\tau_1$. This expression agrees with that obtained by Carr and Purcell and later by Torrey for such pulse sequences. The expressions for the image echo at maximum amplitude, as obtained by different theoretical approaches, have been shown in Table II. The disagreement observed is expected since some of the earlier methods were not rigorously correct, and we discuss them below.

Herzog and Hahn (1956) have extended their method, used in solids, to the case of liquids. If, however, one uses the Eqns. (23) and (25) of their paper to calculate the amplitude of the free precession signals in liquids, one obtains infinite amplitude for the signals*. The reason for this can be seen to be the assumption

$$P(\eta_0) = \text{constant}.$$

Moreover, the above assumption does not represent the physical situation. Also the diffusion-process in liquid can not be described in exactly the same way as

* The equations in the appendix of Herzog and Hahn's paper giving the signal amplitudes in liquids show finite amplitude since the integration was not fully carried out. Actually they should get, for example, $E_{max} \sim \exp\left[-\frac{2}{3} k\tau^3\right] \delta(o)$ for the primary echo, where $\delta(o)$ is the Dirac's δ-function for the zero value of the parameter i.e. at $t = 2\tau_1$. Similar will be the case with other signals.

TABLE II

Expressions for the amplitude of the image echo at echo maximum, according to different theoretical approaches. θ denotes the time of occurrence of the echo maximum, measured from the third puse i.e., $\theta = \tau_2 - 2\tau_1$. $\tau = \tau_2 - \tau_1$ where τ_1 and τ_2 are positions of the second and the third pulses respectively. Echo maximum occurrs at $t = 2(\tau_2 - \tau_1)$ znd ξ_1, ξ_2 and ξ_3 are the nutational angles of the applied pulses as in Table I.

	Common part of the echo-amplitude, as given by different theoretical approaches	Part dependent on diffusion
1. Hahn	$-M_0 \sin\xi_1 \sin^2(\xi_2/2) \sin^2(\xi_3/2) \times \exp\left[-\frac{2(\tau_2-\tau_1)}{T_2}\right]$	$\exp\left(-\frac{8}{3}k\tau^3\right)$
2. Das and Saha	,,	$\exp\left[-k\left\{\frac{5}{3}\tau^3 - 4\tau^2\theta + 5\tau\theta^2 - \theta^3\right\}\right]$
3. The present treatment*	,,	$\exp\left[-2k\left\{\frac{1}{3}\tau^3 - \tau^2\theta + \tau\theta^2\right\}\right]$

* The same results can be also derived from Torrey's (1956) treatment based on the solution of diffusion equation.

they have done in the case of solid. The stationary distribution as obtained from "the probability distribution for the frequency" (see Eq. (31) of their paper) reduces to zero as $t \to \infty$. Their treatment will be valid in the case of liquid also if the probability distribution for the frequency is taken in such a way that it conforms with the actual stationary distribution in liquids. We, however, note that the damping terms in equations for the free precession signals in liquids as given in their paper are identical with ours. This is because the damping terms depend on the probability distribution for the frequency (transition probability) and on the phase factor coming through the solution of the Bloch equations; and these are the same both in our treatment and in Herzog and Hahn's.

The treatment of Das and Saha contains the following important points :—

(1) They assigned definite phase (as they termed) and the Larmor frequency change for each of the free precession intervals. In essence it is equivalent to the splitting up of the actual phase accumulated in any free precession interval into two parts :-

(a) the phase accumulated when the Larmor frequency remains constant in the interval considered, and

(b) the difference between the total phase accumulated and the part described in (a).

In averaging these phase accumulations, they have separately averaged over the two parts considering them to be following independently the Gaussian distribution law. The justification for such treatment is yet to be shown.

(2) They separately considered the phase accumulations in the different free precession intervals. This is not justified for the following reasons :

(a) since the accumulated phase does not follow the Markoff process, the averaging of phase in successive free precession intervals comprising the total interval is not justified.

(b) since the echo signals are made possible due to the preservation of the phase-memory by the nuclear magnets, the consideration of the phase accumulations in different free precession intervals as completely independent does not conform with the physical situation.

Since they considered phase averaging in this way, the phase-reversal could not be taken into account in their treatment.

III. APPARATUS

The apparatus used has been reported earlier by Banerjee *et al.* in this journal (Banerjee *et al.*, 1957). The addition to the apparatus is a trigger generator of conventional type. In order to use Carr-Purcell method for determining relaxation time T_2, a Carr-Purcell sequence generator has been constructed. This is based on the principle of running an one-shot multivibrator with arrangement for a proper positive triggering feed-back through a feed-back amplifier. The total delay is, however, distributed over two such multivibrators in series which also makes it possible to arrange such that the multivibrators return to their initial conditions each time before being triggered. The sequence can be stopped by closing down the feed-back loop by another pulse synchronized with the repitition period generator. This is a very simple method of getting such pulse sequence with fairly good stability of pulse separations. The stability of the multivibrators can be easily improved by increasing the value of the grid-resistor (returning to high tension) in comparison to the plate-load. The circuit for Carr-Purcell sequence generator is shown in Fig. 1.

IV. EXPERIMENTAL PROCEDURE AND RESULTS

(a) *Measurement of Molecular Self-diffusion Co-efficient D :*

For the measurement of D, we observe the amplitude of the "image echo" which is formed at time, $t = 2(\tau_2 - \tau_1)$ with a 90°—180°—180° pulse sequence, and as seen from the expressions in Table II, the relaxation damping of the echo-amplitude will not change with variation of τ_1, if $(\tau_2 - \tau_1)$ is kept constant, whereas the diffusion damping will change. Thus we can isolate the diffusion damping from that due to relaxation. The diffusion damping of this echo can be displayed on the oscilloscope screen by triggering the sweep with a trigger-pulse which changes its

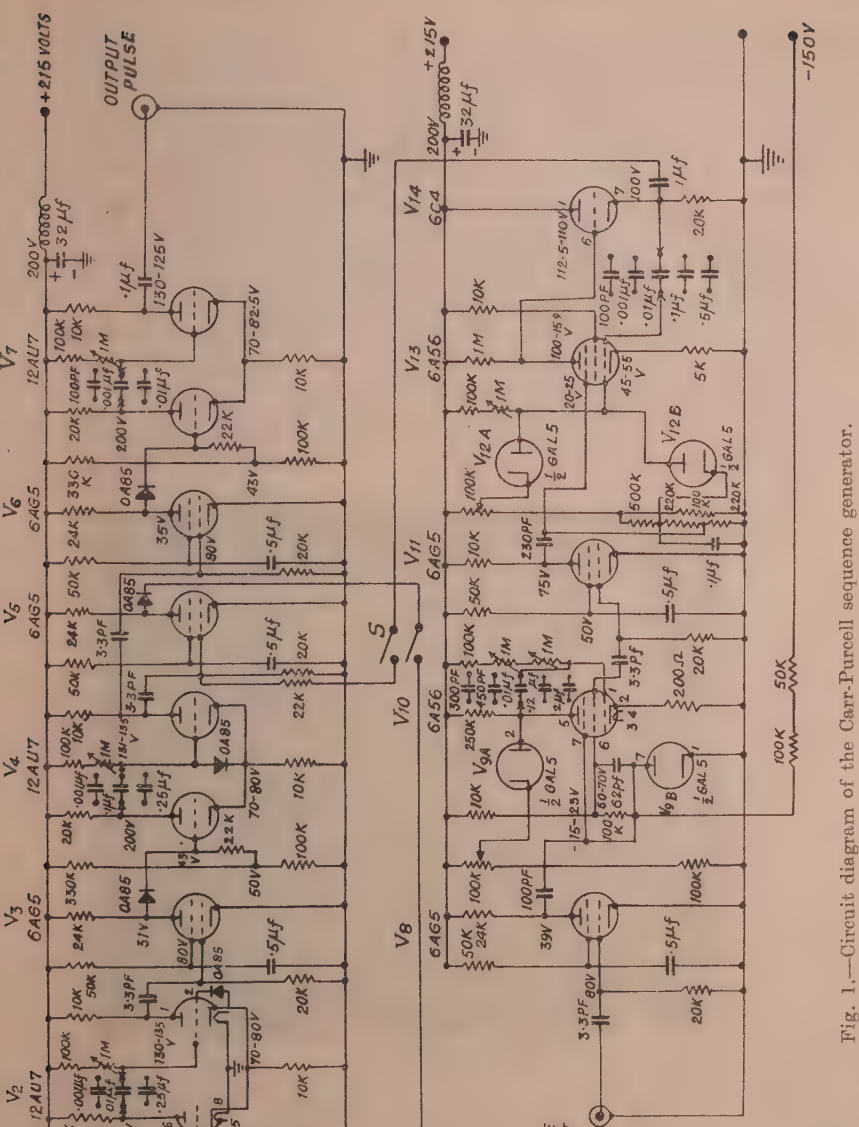

Fig. 1.—Circuit diagram of the Carr-Purcell sequence generator.

position on the time-scale as the value of τ_1 is varied. In practice, the sweep was triggered just before the third pulse by introducing a fixed delay between the second pulse and the triggering pulse. Hence as τ_1 was changed keeping $(\tau_2-\tau_1)$ constant, the triggering pulse also correspondingly changed its position, the small delay between the triggering and the third pulse, however, always remained the same. One can now obtain a multiple exposure of this echo with variation of τ_1. With the above arrangement, where the position of the image-echo is kept constant (by keeping $(\tau_2-\tau_1)$ constant), and the position of the triggering pulse is shifted exactly by the same amount as the variation in τ_1, we get a plot of the echo-amplitude *vs.* $\theta\,[=2(\tau_2-\tau_1) \quad \tau_2 \quad \tau_2-2\tau_1]$, θ denoting the time measured from the 3rd pulse. The triggering of the sweep was done by a pulse from a trigger-generator which is itself triggered by the second pulse such that the delay between the second and the triggering pulse can be kept constant. Fig. 2 shows such a multiple exposure.

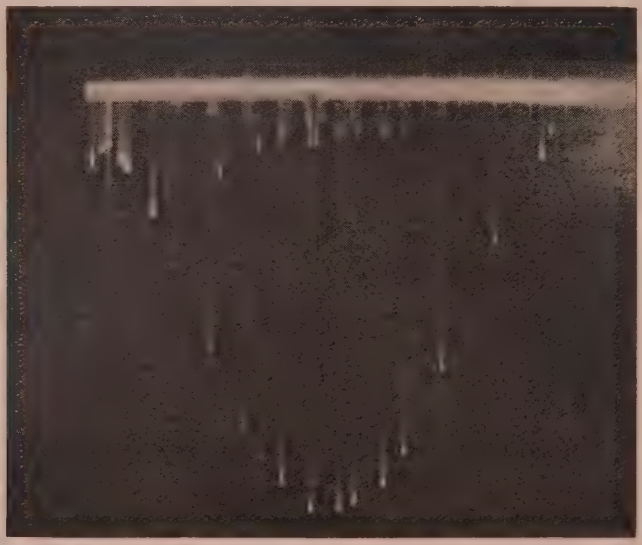

Fig. 2.—Multiple exposure of the image echo from protons in water, with variation of τ_1, keeping $(\tau_2-\tau_1)$ constant. A sequence of three pulses $(90^\circ\text{-}180^\circ\text{-}180^\circ)$ applied at times $t=0$, τ_1 and τ_2 respectively has been used. The sweep calibration with 2ms marker can be seen below the base-line.

The use of $90^\circ-180^\circ-180^\circ$ pulse sequence with exact values of these angles is not critical, but the angle adjustments are done as accurately as possible in order to minimise the amplitudes of all other echoes which may interfere on the multiple-exposure photograph. A preliminary check is made to see that the resonance condition is reached (Ghose *et al.*, 1957*a*), the maintenance of the resonance condition being also not essential. It is, however, essential to maintain the mag-

netic field H_0 at a constant value. This was done in our case with the help of a flourine signal, obtained by steady NMR method.

As seen in Table II, the plot of $\log_e A$ *vs.* θ ($\tau_2 - 2\tau_1$) where A is the echo-amplitude, is a parabola satisfying the equation

$$\log_e A = \text{constant} + 2k\tau^2\theta - 2k\tau\theta^2 \qquad \ldots \quad (14)$$

where $\tau = \tau_2 - \tau_1 = \text{constant}$. Thus k can be obtained from the experimental data fitting them to an equation of parabola by the standard method (Johnson, 1952) and comparing the latter with relation (14). Such a parabola is shown in the Fig. 3. k can also be evaluated from the gradients of (14) at $\theta = 0$ and $\theta = \tau$, since

$$\left[\frac{d}{d\theta}\log_e A\right]_{\theta=0} = -\left[\frac{d}{d\theta}\log_e A\right]_{\theta=\tau} = 2k\tau^2 \qquad \ldots \quad (15)$$

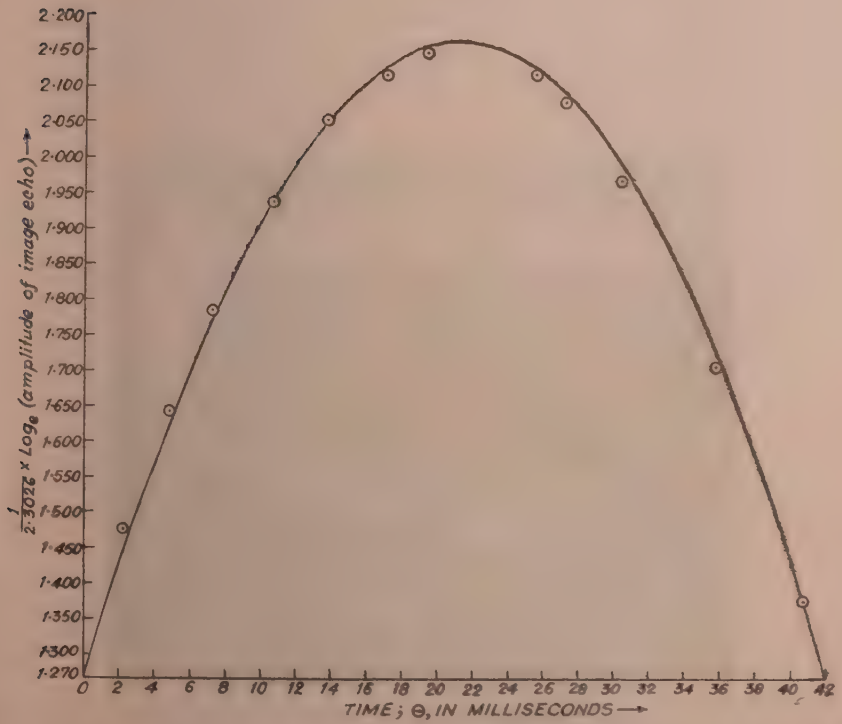

Fig. 3. The logarithm of the amplitudes of the image echo is plotted against θ, given by $\theta = \tau_2 - 2\tau_1$, where τ_1 and τ_2 give the position of the second and the third pulse respectively. The parabola fitting the experimental points are also shown (in solid line).

From the geometry of the parabola, this gradient can be evaluated simply from the relation

$$\left[\frac{d}{d\theta}\log_e A\right]_{\theta=0} = \frac{2\{(\log_e A)_{\theta=\tau/2} - (\log_\theta A)_{\theta=0}\}}{\tau/2} \quad \ldots (16)$$

Combining (15) and (16)

$$k = \frac{2\{(\log_e A)_{\theta=\tau/2} - (\log_e A)_{\theta=0}\}}{\tau^3} \quad \ldots (17)$$

To obtain D from the value of k, the magnitude of the magnetic field gradient, G, is required. The magnetic field gradient was applied as was suggested by Carr and Purcell by two co-axial coils of 170 turns each wound on a perspex form, the common axis of the coils being in the direction of H_0. The value of G was experimentally determined from the echo modulation. By considering in some cases six or seven such maxima or minima it was found that the maximum deviation from the average value of G as determined from the different maxima or minima was 3 to 4% at most, which indicates that the over-all field gradient along the axis of the sample holder was negligible.

The *rf* field H_1 used was approximately 5 gauss, and the proton resonance was observed at about 14 mc/sec.

D was measured with three different field gradients, 1.19, 1.71 and 2.18 gauss/cm, and was found to be the same within experimental error, the average

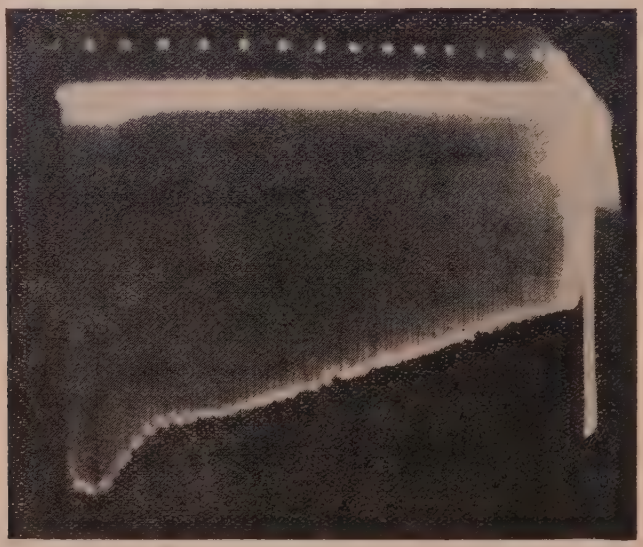

Fig. 4.—Carr-Purcell echoes from protons in water, with the magnetic field gradient 1.71 gauss/cm, almost from the beginning of the sequence. The value of τ, the separation between the first 90° and the next 180° pulses, used was 3.3 ms. Sweep calibrator marker separation was 40 ms.

value being 2.6×10^{-5}cm^2/sec for water at room temperature (30°C). The sample was doubly distilled water sealed in a pyrex glass-tube. The value of D thus determined agrees well with other measurements [Carr and Purcell (1954), Orr and Bulter (1935), Wang *et al.* (1953)].

(*b*) *Measurement of* T_2 *:*

If k is known the value of T_2 can be determined in principle by Hahn's method, where the two pulse echo amplitude is corrected for diffusion damping and plotted against τ_1, the slope of the resulting straight line giving $1/T_2$. In case of protons in water the value of T_2 is comparatively large, and thus the slope will be small. Thus in this case time considered should be made large. But it was found that for large values of time, the corrected echo-amplitudes do not fall on a straight line, the expected straight line showing oscillatory tendencies (giving maxima and minima with increase of time). The origin and the nature of this phenomenon is being investigated in greater details.

T_2 can, however, be determined accurately from Carr-Purcell decay constant after correcting it for diffusion damping. Even for large field gradient, this correction gives good result for the value of T_2. Fig. 4 shows a photograph of Carr-Purcell sequence of echoes for water, the magnetic field gradient used was 1.71

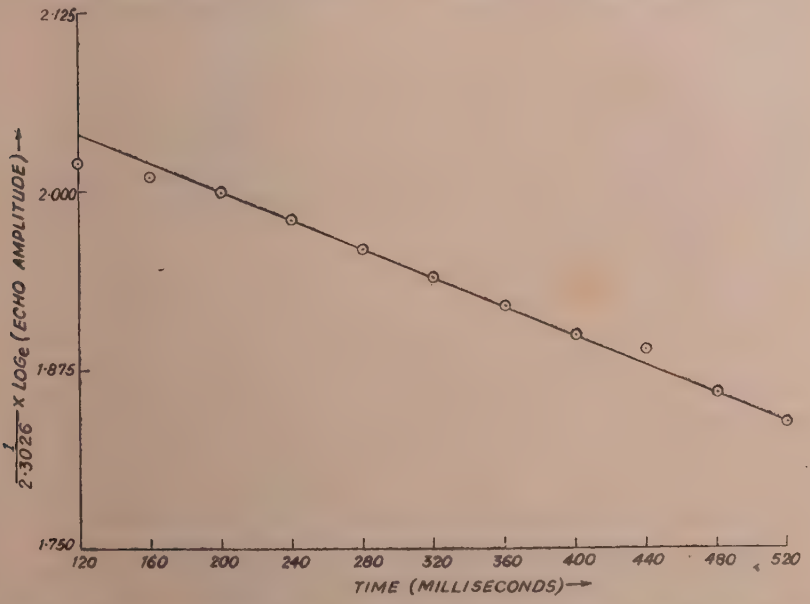

Fig. 5.—The logarithms of the echo amplitudes obtained from the Carr-Purcell sequence (Fig. 4) are plotted against time. The slope of the straight line gives $\frac{1}{T_2{}^*} = \frac{1}{T_2} + \frac{1}{3} k\tau^2$ where $k=\gamma^2G^2D$ and τ is the separation between the first 90° and the next 180° pulses From this, T_2 can be obtained, if k and τ are determined separately.

gauss/cm. In Fig. 5 the logarithms of the echo-amplitudes are plotted against time. The value of the envelope decay constant, T_2^* as obtained from Fig. 5, which is related to T_2 by the following relation

$$\frac{1}{T_2^*} = \frac{1}{T_2} + \frac{1}{3} k\tau^2 \qquad \ldots (18)$$

where τ is the separation between the 1st 90° pulse and the next 180° pulse, is found to be 1.99 seconds. Using the previously determined value of k and τ, the value of T_2 comes out as 2.5 seconds.

With the same sample of water, T_1 also was determined by null method (Ghose *et al.*, 1957b), and was found to be 2.88 seconds, thus the ratio of T_1/T_2 agrees well with BPP theory (Bloembergen *et al.*, 1948).

In the above determinations the error creeps in mainly because of the following causes :

(1) Very high degree of stability in the delays introduced by the multivibrators, in our pulsing system, cannot be expected, because of inherent instability of such systems.

(2) The accuracy in time measurement is also limited as we had to calibrate the oscilloscope sweep by an external marker (Hewlett Packward, Model 100D and 202A). Even with very stable marker the time-measurement will not be correspondingly accurate since one has to measure time from the calibration of the oscilloscope sweep.

(3) The noise-figure of the apparatus limits the accuracy of measurement of the signal amplitudes and the error due to this cause is difficult to estimate exactly.

The use of scalar-type pulsing arrangement with stable oscillators as time-generators will remove the causes (1) and (2) to a large extent, and thus will improve the accuracy of measurement.

It is, however, expected that the maximum error in all our determinations was less than 5%.

(c) *Experimental check of the different theoretical approaches*

So far, the value of D, as obtained using the different theoretical formulations, was considered as a check of the theoretical approaches. This is, however, indirect. The "image" echo considered in the present work affords a direct check since the nature of variation of its amplitude with θ, is predicted to be different in different approaches. According to Hahn's approach the amplitude of this echo should not change at all. This approach is then obviously not correct, which was modified later by Herzog and Hahn*. According to Das and Saha's treatment the amplitude of this echo follows the following equation

$$\log_e A = \text{constant} + 4k\tau^2\theta - 5k\tau\theta^2 + k\theta^3 \qquad \ldots (19)$$

* However, their results for liquids are not considered here for reasons explained in Section II.

and the maximum of $\log_e A$ will occur at

$$\theta = 0.465(\tau_2 - \tau_1)$$

According to the present approach, the above maximum will be at

$$\theta = 0.5(\tau_2 - \tau_1)$$

There is thus about 7% difference in the predicted positions of the maximum. Experimental results on the determination of the position of this maximum favour the conclusion of the present paper. In Fig. 6 Eqns. (14) and (19) are plotted in a scale such that they are closest to each other. The experimental points are then reduced to the same scale to observe which of the two curves they follow. It is found that they follow the Eq. (14) more closely than the Eq. (19) showing that the present approach is more acceptable.

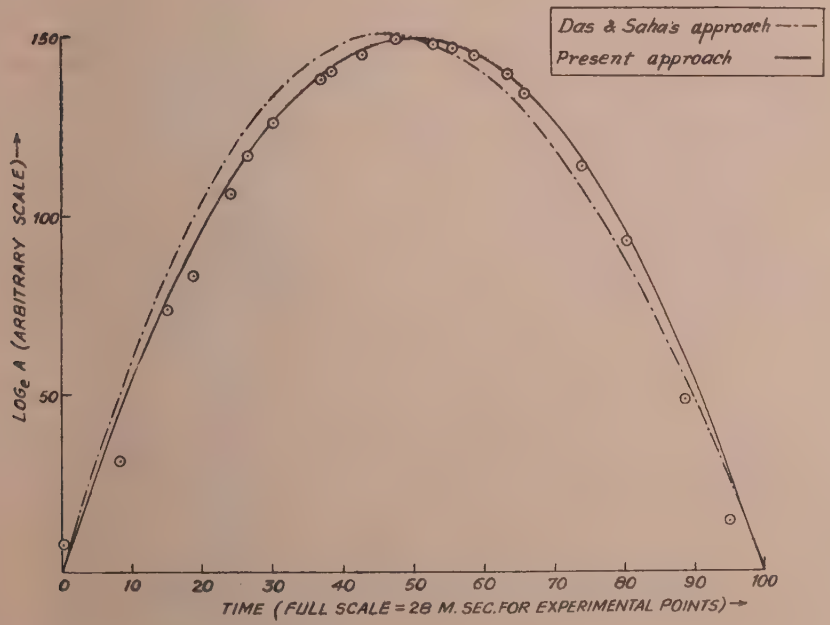

Fig. 6.—The theoretical Eqns. (14) and (19), giving the logarithms of the amplitude of the image echo, as derived from Das and Saha's and from the present treatment are drawn in the same scale for comparison with the experimental data, which are also plotted here in the same scale. The Eqns. (14) and (19) are brought to the same scale by coinciding any two points of the two curves. The two corresponding experimental points are then brought to those common points for reducing the experimental points to the common scale of the two curves.

V. DISCUSSION

Let us now examine the various different NMR methods for the measurement of D and T_2. Of all such methods*, those developed by Hahn and by Carr and Purcell are mostly used.

Hahn's method of measurement of T_2 is seriously handicapped in most cases where the liquids have comparatively small viscosity. In these cases even in most homogeneous magnets ordinarily available, the diffusion effect will seriously interfere with the measurement of T_2.

Carr-Purcell's method removes this difficulty by minimizing the diffusion-effect, for which one has to use a large number of 180° *rf*-pulses. If the adjustment of the angles of the 180° *rf*-pulses is not exact, the error produces a cumulative effect and the amplitude of the echo formed after a large number of pulses becomes seriously affected. It can, however, be shown that if the echoes after a large number of pulses are considered the above effect introduces an extra damping such that the total damping remains still exponential. This extra damping can be made negligibly small if the error in the adjustment of the angle of the 180° -pulses is kept within 1-2%. This can be easily obtained. One should, however, note that Meiboom and Gill (1958), have suggested a method by which the above cumulative error can be reduced. But in general case, the overall field inhomogeneity and the values of relaxation time T_2 may prevent the use of a large number of *rf*-pulses, which thus limits the application of the method in such cases. One can, however, adjust the field gradient such that the exponential decay of the Carr-Purcell echo sequence contains only the diffusion and the relaxation damping, the relaxation time can then be accurately determined from that decay constant, if the diffusion damping at the field gradient is ascertained independently. This is exactly what is done in the present method as described in Section IV.

We also note that while determining D from Hahn's plot (after finding out T_2 previously) Carr and Purcell found that with large field gradients there is departure from the expected straight line. This effect also limits the use of Carr-Purcell method for measuring D in general cases. Similar departure from the straight line was also observed when we attempted to evaluate T_2 from Hahn's plot, after finding out $k(= \gamma^2 G^2 D)$ previously. As mentioned earlier in Section IV, we obtained a curve showing maxima and minima, instead of a straight line. This effect shows itself at large time t and increases with the increase in the value of the field gradient. Both the Carr-Purcell and the Douglas-McCall methods of measuring D from Hahn's plot will be seriously affected by the above phenomenon. In the present method this effect can be made very small even for large magnetic

* A brief account and the references of different methods of measuring T_2 can be found in "Nuclear Magnetic Resonance" by E. R. Andrew, Cambridge University Press, London (1955).

field gradient by properly adjusting the separation between the second and the third pulses, such that diffusion-damping becomes predominent in comparison with the above effect.

Though the effect of chemical shift and J-coupling (Hahn and Maxwell, 1952) will affect the amplitude of the image echo, their effect can be minimized in the present method by properly choosing the value of the magnetic field gradient. It may be mentioned here that the previous determination of D can be profitably used in the evaluation of J by the spin-echo technique (Hahn and Maxwell, 1952 and Crawford and Foster, 1956)].

ACKNOWLEDGMENTS

The authors wish to thank Prof. A. K. Saha and Mr. B. M. Banerjee for their encouragement and interest during the progress of the work. They also appreciate many helpful discussions and cirticism from Dr. D. K. Roy and Mrs. T. Roy.

REFERENCES

Anderson, P. W., 1954, *J. Phys. Soc., Japan*, **9**, 316.
Banerjee, B. M., Ghosh, S. K. and Saha, A. K., 1957, *Ind. J. Phys.*, **31**, 211.
Bloch, F., 1946, *Phys. Rev.*, **70**, 460.
Bloembergen, N., Purcell, E. M. and Pound, R. V., 1948, *Phys. Rev.*, **73**, 673.
Carr, H. Y. and Purcell, E. M., 1954, *Phys. Rev.*, **94**, 630.
Chandrashekhar, S., 1943, *Rev. Mod. Phys.*, **15**, 1.
Crawford, G. J. R. and Foster, J. S., 1956, *Canad. J. Phys.*, **34**, 653.
Das, T. P. and Saha, A. K., 1954, *Phys. Rev.*, **93**, 749.
Douglas, D. C. and McCall, D. W., 1958, *J. Phys. Chem.*, **62**, 1102.
Ghose, T., Ghosh, S. K. and Roy, D. K., 1957a, *J. Phys. Soc., Japan*, **12**, 816.
Ghose, T., Ghosh, S. K. and Roy, D. K., 1957b, *Nuovo Cimento Series* X, **6**, 1771.
Green, H. S., 1952, "The Molecular Theory of Fluids ," North-Holland Publishing Company, Pages 195 ff.and 151 ff.
Hahn, E. L., 1950, *Phys. Rev.*, **80**, 580.
Hahn, E. L. and Maxwell, D. E., 1952, *Phys. Rev.*, **88**, 1070.
Herzog, B. and Hahn, E. L., 1956, *Phys. Rev.*, **103**, 148.
Inc., New York, Chapter Nine.
Johnson, Lee H., 1952, Nomography and Empirical Equations. John Wiley & Sons.
Kirkwood, J. G., 1946, *J. Chem. Phys.*, **14**, 180.
Meiboom, S. and Gill, D., 1958, *Rev. Sci. Instr.*, **29**, 688.
Orr, W. J. C. and Butler, J. A. V., 1935. *J. Chem. Soc.*, 1273.
Rabi, I. I., Ramsey, N. F. and Schwinger, J., 1954, *Rev. Mod. Phys.*, **26**, 167.
Torrey, H. C., 1956, *Phys. Rev.*, **104**, 563.
Wang, J. H., Robinson, C. V. and Edelman, I. S., 1953, *J. Amer. Chem. Soc.*, **75**, 466.
Wang, M. C. and Uhlenbeek, G. E., 1945, *Rev. Mod. Phys.*, **17**, 323.

40

ABSORPTION OF MICROWAVES IN CYCLOHEXANOL AND CYCLOPENTANOL AND THEIR SOLUTIONS

T. J. BHATTACHARYYA

Optics Department, Indian Association for the Cultivation of Science, Jadavpur, Calcutta 32.

(*Received, June* 20, 1960)

ABSTRACT. The absorption of 3.18 cm microwaves in cyclohexanol, cyclopentanol, and their solutions in heptane and carbon tetrachloride was studied at different temperatures. The solution in CCl_4 did not show any absorption. The temperature-attenuation curves show maxima at 105°C, 96°C, 14°C and 8°C respectively in the cases of cyclohexanol, cyclopentanol and 10% solutions of the substances in heptane. The values of the radius of the rotor calculated from Debye's theory are 1.41, 1.42, 1.40 and 1.43Å respectively. The rotor has been identified with the OH group.

The attenuation coefficients for the solutions in heptane were found to be greater than those of the pure liquids. This has been explained on the assumption that in pure liquids there exist dimers formed through intermolecular OH..O bond which break up in the solutions.

The absence of any absorption in the solutions of CCl_4 has been attributed to the formation of OH..Cl bond between the solvent and the solute molecules.

INTRODUCTION

The study of the absorption of microwaves of wavelength 3.18 cms in *o*-chlorophenol (Ghosh, 1955) and in solutions in CCl_4 (Bhattacharyya, 1958) and similar investigations in ethylene chlorhydrin (Bhattacharyya, 1959) furnished evidence for the formation of hydrogen bond between neighbouring molecules in the pure liquids and breaking up of such associated groups into single molecule in solutions in suitable solvents. In the case of solution of ethylene chlorhydrin in methyl cyclohexane it was found that of the two types of dimers present in the liquid only those formed through the intermolecular OH...O bond break up into single molecules in the solution. There was no further interaction between solvent and the solute molecules, but in the case of the solution in CCl_4 it was found that an intermolecular OH...Cl bond is formed between the solvent and the solute molecules so that the C—Cl group at the other end of the latter molecule possesses freedom of rotation about the C—Cl bond. These results confirmed the conclusions drawn by Mazumder (1959) from the results of investigations of the infrared spectra of the solution of ehylene chlorhydrin in CCl_4.

It was thought worthwhile to extend the investigation to other substances containing OH group as a substituent. Cyclopentanol and cyclohexanol which are two typical alicyclic alcohols were chosen for this purpose and the absorption of 3.18 cm microwaves in solutions of these two compounds in heptane and carbon tetrachloride has been investigated.

EXPERIMENTAL

The experimental arrangements and procedure were similar to those used in a previous investigation (Bhattacharyya, 1958).

In order to verify whether the absorption observed with any particular cell was genuine or spurious, two cells of different thicknesses were used successively and the strengths of absorption in the two cells were compared. The absorption was studied in the pure liquids and also in 10% solutions of the liquids in CCl_4 and in heptane. The values of the static dielectric constants, the refractive indices and the coefficients of viscosity for the pure liquids were obtained from the standard tables. As the data for solution in heptane were not available they were determined experimentally. In the case of the solutions in CCl_4 no absorption of the microwaves was observed.

The radius of the rotor, a, was calculated in the case of the pure liquids with the help of the Debye's formulae :

$$\omega\tau = \frac{\epsilon_0+2}{\epsilon_1+2}\sqrt{\frac{\epsilon_1}{\epsilon_0}} \; ; \; a^3 = \frac{KT}{4\pi\eta} \qquad \ldots \quad (1)$$

where ϵ_0, the dielectric constant at very high frequencies has been taken to be the square of the refractive index of the liquid, ϵ_1 and η are the dielectric constant and the coefficient of viscosity of the liquid at the temperature $T°K$ at which the maximum absorption of the 3.18-cm waves takes place.

In the case of the solution in heptane also the same formulae and the constants determined experimentally were used.

RESULTS AND DISCUSSION

The temperature-dependence of the attenuation coefficient for the pure liquids has been shown in Fig. 1. Curves I and II are for two different cells filled with pure cyclopentanol. Similarly, curves III and IV show the absorption in pure cyclohexanol in the two cells.

Fig. 2. shows the relation between temperature and the attenuation coefficient for the 10% solutions of the cyclopentanol and cyclohexanol in heptane. In calculating attenuation coefficient for the solutions, the equivalent thickness of the substance in the cell instead of the real thickness of the cell has been taken into consideration.

The radius of the rotor calculated for the different samples are given in Table I. It is found to be about 1.4×10^{-8} cm in each case. The temperatures at which the maximum absorption take place in cyclopentanol and cyclohexanol are 96°C and 105°C respectively. From Fig. 1 it is observed that the two cells of different thickness give identical results which show that the absorption is genuine.

TABLE I

Substances	$\omega/2\pi$ Mc/sec.	ε_1	$\sqrt{\varepsilon_0}$	$\tau \times 10^{11}$/sec	100η	T°K	$a \times 10^8$ cm
Cyclo-pentanol	9415	9.00	1.45	1.31	1.90	369	1.42
Cyclo-hexanol	„	8.00	1.46	1.35	2.06	379	1.41
10% soln. of cyclo-pentanol in heptane	„	6.00	1.43	1.48	1.70	281	1.40
10% soln. of cyclohexanol in heptane	„	5.00	1.44	1.51	1.65	287	1.43

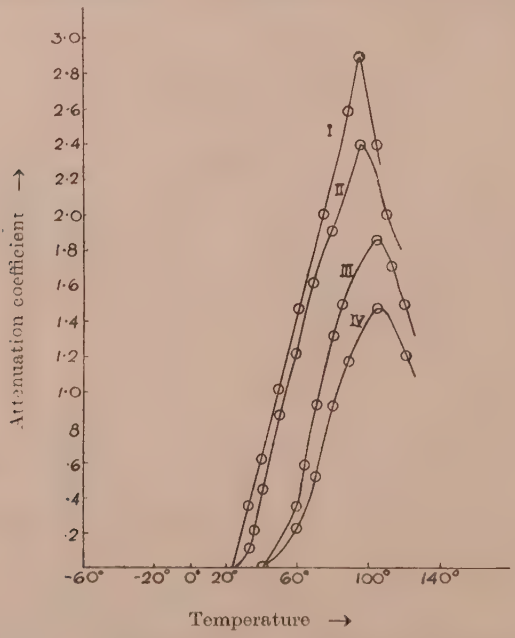

Fig. 1. Curve I—Pure cyclopentanol, thickness of the liquid = 1.4 cm.
Curve II— „ „ „ „ = 1.0 cm.
Curve III—Pure cyclohexanol, thickness of the liquid = 1.4 cm.
Curve IV— „ „ „ „ = 1.0 cm.

The fact that the solutions in heptane show the maximum absorption of the microwaves at much lower temperatures also lends additional support to the conclusions that the absorption is genuine and that it is dependent on the viscosity of the liquid, as postulated in Debye's theory. These results further show that Debye's formula is applicable in these cases.

From Fig. 2 it is observed that the values of the maximum attenuation coefficient for the solutions of cyclohexanol and cyclopentanol in heptane are 8.9 and 12.0 respectively. Fig. 1 on the other hand shows the maximum values in the case of pure cyclohexanol and cyclopentanol to be 1.84 and 2.88 respectively. The increase of absorption in the case of the solutions indicates the increase of the free OH group in solutions. Hence it can be concluded that the OH group in large number of molecules in the pure substances have no freedom of orientation. This can only happen if associated pairs of molecules are formed through intermolecular OH...O bonding. It can therefore be concluded that in the pure alcohols loose dimers are formed through intermolecular OH...O bond and they break up into single molecules in solutions.

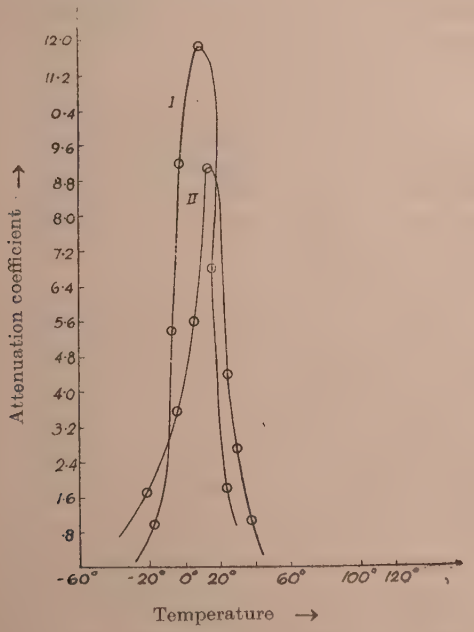

Fig. 2. Curve I—10% solution of cyclopentanol in heptane, (thickness of the cell = 1.4 cm.)
Curve II—10% solution of cyclohexanol in heptane, (thickness of the cell = 1.4 cm.)

In solutions in carbon tetrachloride, however, no absorption was observed though the viscosity of the solution in CCl_4 is nearly the same as that of the

solution in heptane. It might be expected that the OH...O bond should break up in these solutions. Hence the absence of absorption indicates the formation of a new type of hydrogen bond due to the action of the solvent molecules. It is quite probable that the OH group of the molecule of either of the compounds forms virtual linkage with the chlorine atom of the CCl_4 molecule in the solutions. This newly formed OH...Cl bond prevents the free orientation of the OH group and consequently, no absorption of the microwaves can take place in these solutions. Evidence for the formation of such OH...Cl bond between the solvent and solute molecules in the solution of ethylene chlorhydrin in CCl_4 was observed earlier (Bhattacharyya, 1959). Study of the infrared absorption of the solution of ethylene chlorhydrin in CCl_4 (Mazumder, 1959) also led to these conclusions.

The results of these investigations thus throw much light on the nature of influence of intermolecular fields in such polar liquids and their solutions in suitable solvents.

ACKNOWLEDGMENT

The author is indebted to Professor S. C. Sirkar, D.Sc., F.N.I., for his constant guidance throughout the progress of the work.

REFERENCES

Bhattacharyya, T. J., 1958, *Ind. J. Phys.*, **32**, 573.
,, ,, 1959, *Ind. J. Phys.*, **33**, 498.
Ghosh, D. K., 1955, *Ind. J. Phys.*, **29**, 450.
Mazumder, M. M., 1959, *Ind. J. Phys.*, **33**, 346.

41

LIGHT ABSORPTION IN PARAMAGNETIC IONS IN STATE OF SOLUTION. PART II—Ni^{++} ION

A. MOOKHERJI AND N. S. CHHONKAR

PHYSICS LABORATORIES, AGRA COLLEGE, AGRA

(*Received, June* 10, 1960)

ABSTRACT. The light absorption in aqueous solution of nickel salts are studied in the range 10,000 Å to 3900 Å by a Hilger Uvispek spectrophotometer and the results are discussed in the light of crystalline electric field theory.

The cubic field coefficient has almost the same value in all the salts except the amino-salts.

It is observed that the term separation comes to be smaller for the ion in crystal than for the free ion. From this lowering the covalency factor f^2 was evaluated. f^2 tends to a value of 0.9 for all the salts except the amino-salts pointing that $f_\pi{}^2$ is unity in them. In amino-salts f^2 arises from σ — and π— orbital overlap.

Excellent agreement with the measured values of magnetic anisotropy was obtained by attributing the bands at 13,900 cm^{-1} and 15,200 cm^{-1} as due to the splitting by a crystal field of tetragonal symmetry.

The effect of long range field was observed to be very pronounced in single sulphate and salenate, double sulphates and selenates of K and Rb, while this was less pronounced in double sulphates and selenates of NH_4 and Tl.

INTRODUCTION

In the previous part of this paper (Mookherji & Chhonkar, 1959) which we shall refer as part I hereafter, a systematic optical investigation of the consequences of the crystalline electric fields on cupric ions in about twenty different salts in state of aqueous solution has been reported. A number of interesting results that have been obtained are :

1) At least some of the co-ordinating members of the octahedral cluster about the Cu^{++} ion in some salts are very probably other than water molecules.

2) The complex, $[Cu(H_2O)_6]^{2+}$, in different salts in aqueous solution is not truely ionic but possesses some amount of covalent bonding.

3) In some salts appreciable σ-bonding prevails and π-bonding is neglected, while in others there are both σ-orbital and π-orbital overlap.

4) The position of the absorption bands in state of solution does not vary much from salt to salt amongst sulphates, nitrates, chlorides etc.; while there are appreciable variations amongst others (i.e. acetate, propionate and formate).

For free Cu^{++} ion, the ground state is ^2D; no other terms of the same multiplicity lie very close, whereas for free Ni^{++} ion the ground state is ^3F and a term of the same multiplicity ^3P lies 16,900 cm^{-1} above it (Moore, 1952). Naturally the crystalline field splitting of the ground state of the two free ions will be very different. Just like Cu^{++} ion, in octahedrally co-ordinated salts of Ni^{++} ion, an orbitally non-degenerate level lies lowest in the Stark-pattern, but weaker spin-orbit coupling in Ni^{++} ion makes the contribution from the upper levels to the g- and μ-values appreciably smaller than that for Cu^{++} ion (Owen, 1955; Bose and Mitra, 1952).

Dreisch *et al.* (1937, 1939) working on the selective optical absorption spectra of Ni^{++} ion in $[Ni(H_2O)_6]^{2+}$ and $[Ni(NH_3)_6]^{2+}$ salts observed broad absorption bands with centres at about 8,497 cm^{-1}, 15,370 cm^{-1} and 25.510 cm^{-1} and 10,804 cm^{-1} 17,200 cm^{-1} and 27,900 cm^{-1} respectively. They reported a fine structure of the band at 8,497 cm^{-1}. Owen *et al.* (1957) were unable to find any such fine structure of this band, using much higher resolving power instruments.

Jörgensen (1955) has shown that in a series of Ni^{++} complexes the lowest singlet state intermixes strongly with triplet states giving rise to double bands.

The present communication deals with the measurements of absorption spectra of about twenty nickel salts in aqueous solution. The results are discussed in the light of the theories developed by Hartmann and Müller (1958), Orgel (1955), Jörgensen (1955), Griffiths and Owen (1952) and Owen (1955).

EXPERIMENTAL

The measurements were carried out by Hilger's Uvispek spectrophotometer and the same procedure as in part I of this paper (Mookherji and Chhonkar, 1959) was adopted. Chemicals used were of Merck's gravimetric reagent quality. Triple distilled water was used for making solutions.

The measurements were centred round about 27°C, but no observable change in the position of the absorption bands was noted for small room temperature variations.

RESULTS

The results of the measurements are collected in Tables Ia and Ib. In order to get prominent absorption peaks for the salts studied, the solutions had to be diluted. Just like cupric salts (part I), progressive dilution from that concentration at which the prominent peak is obtained, does not change the position of the bsorption peak. The variations of absorption in different salt solutions are shown graphically in figs. 1 to 18.

TABLE Ia

Salts	Concentrations %	Maximum absorption at					
		λ in Å			Wavenumbers in cm^{-1}		
		II	III	IV	II	III	IV
$NiSO_4$	3	7190	6580	3950	13,910	15,200	25,320
$NiSeO_4$	4	7220	6570	3950	13,850	15,220	25,320
$Ni(NH_4.SO_4)_2$	3	7200	6560	3945	13,890	15,240	25,350
$Ni(K.SO_4)_2$	4	7190	6570	3945	13,910	15,220	25,350
$Ni(Rb.SO_4)_2$	4	7225	6600	3950	13,850	15,150	25,320
$Ni(Tl.SO_4)_2$	sat.	7195	6560	3945	13,900	15,240	25,350
$Ni(NH_4SeO_4)_2$	4	7230	6580	3950	13,830	15,200	25,320
$Ni(K.SeO_4)_2$	4	7230	6580	3950	13,830	15,200	25,320
$NiCl_2$	3	7180	6550	3950	13,980	15,270	25,320
$NiBr_2$	2	7220	6580	3950	13,850	15,200	25,320
$Ni(NO_3)_2$	2	7190	6570	3950	13,910	15,220	25,320
$Ni_3Bi_2(NO_3)_{12}$	4	7240	6600	3945	13,810	15,150	25,350
$Ni(CHOO)_2$	2	7225	6600	3950	13,850	15,150	25,320
$Ni(CH_3COO)_2$	3	7200	6580	3950	13,890	15,200	25,320

TABLE Ib

Salts	Concentration %	Maximum absorption at					
		λ in Å			Wavenumbers in cm^{-1}		
		I	II+III	IV	I	II+III	IV
$[Ni(NH_3)_4](SO_4)$	2.25 1:1 NH_4OH	9500	5785	3600	10,530	17,280	27,780
$[Ni(NH_3)_4](OH)$	1.5 1:1 NH_4OH	9525	5775	3600	10,490	17,310	27,780
$[Ni(NH_3)_4](Cl)$	2.0 1:1 NH_4OH	9350	5750	3600	10,700	17,390	27,780
$[Ni(NH_3)_4](CH_3COO)$	2.0 1:1 NH_4OH	9325	5750	3600	10,720	17,390	27,780

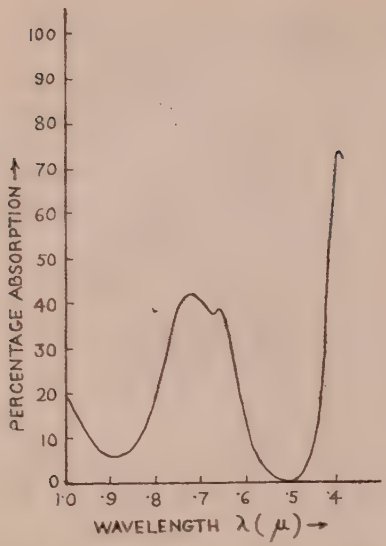

Fig. 1. Stark splitting of ground state of Ni^{++} ion.

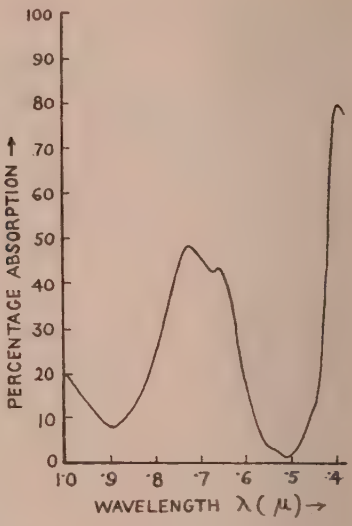

Fig. 2. Absorption curve of 3% $NiSO_4$ solution.

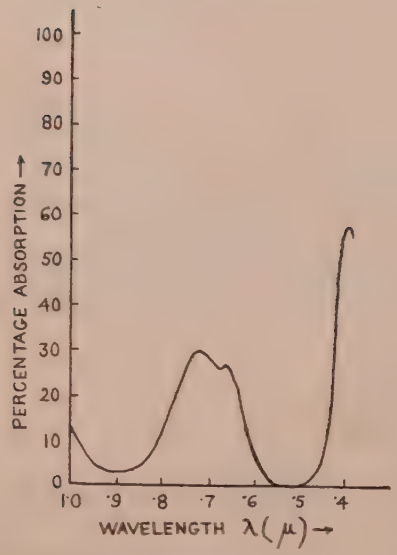

Fig. 3. Absorption curve of 4 % $NiSeO_4$ solution.

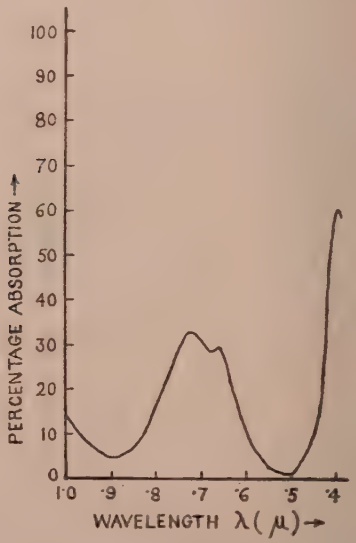

Fig. 4. Absorption curve of 3 % Ni $(NH_4.SO_4)_2$ solution.

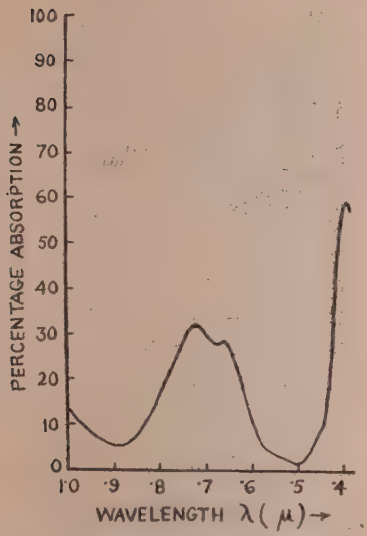

Fig. 5. Absorption curve of 4% $Ni(K.SO_2)_2$ solution

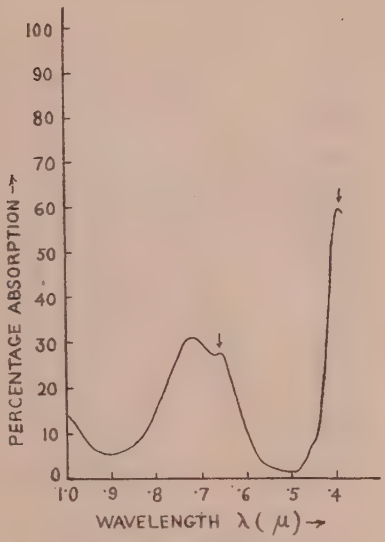

Fig. 6. Absorption curve of 4% $Ni(Rb.SO_4)_2$ solution

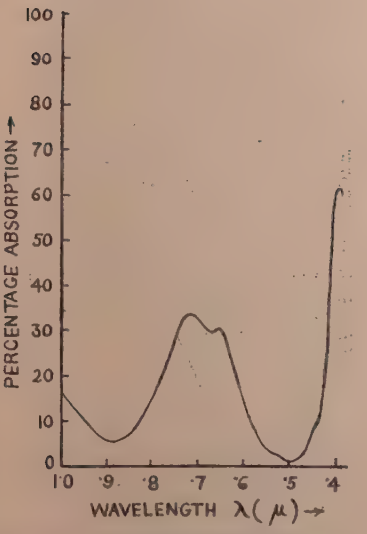

Fig. 7. Absorption curve of sat. $Ni(Tl.SO_4)_2$ solution

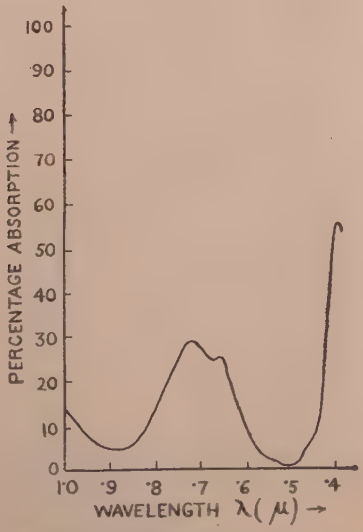

Fig. 8. Absorption curve of 4% $Ni(NH_4,SeO_4)_2$ solution

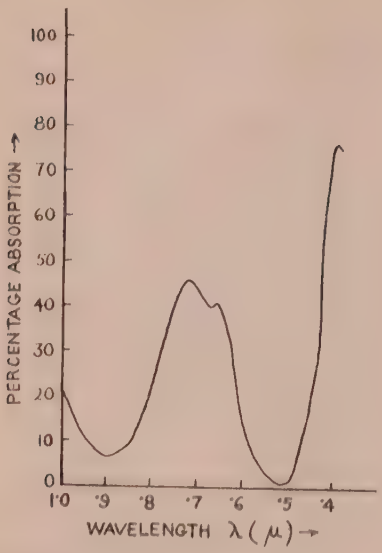

Fig. 9. Absorption curve of 4% $Ni(KSeO_4)_2$ solution

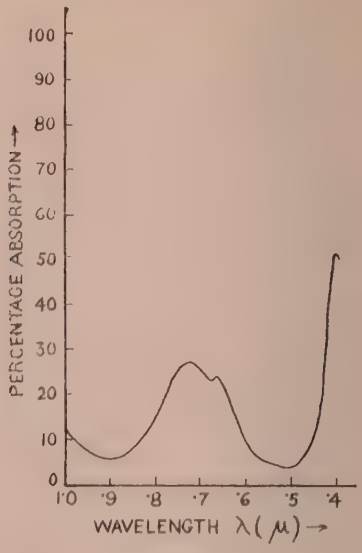

Fig. 10. Absorption curve of 3% $NiCl_2$ solution

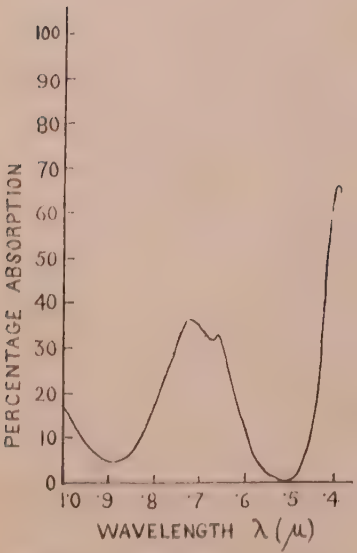

Fig. 11. Absorption curve of 2% $NiBr_2$ solution

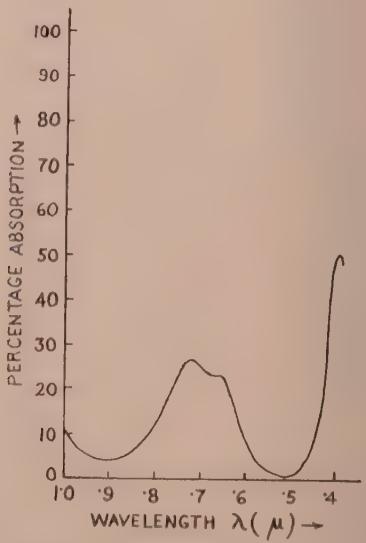

Fig. 12. Absorption curve of 2 % $Ni(NO_3)_2$ solution

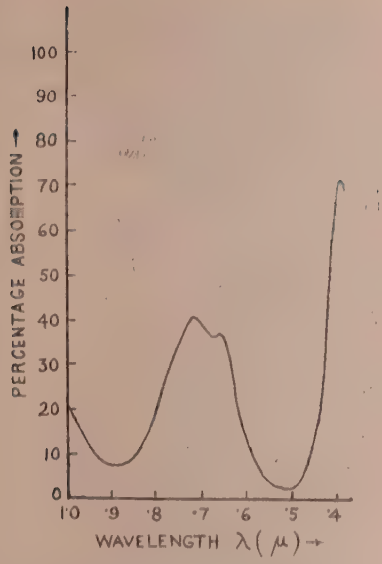

Fig. 13. Absorption curve of 4% $Ni_3Bi_2(NO_3)_{12}$ solution

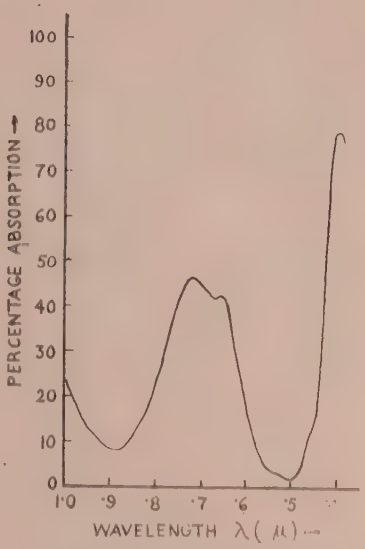

Fig. 14. Absorption curve of 2% $Ni(HCOO)_2$ solution

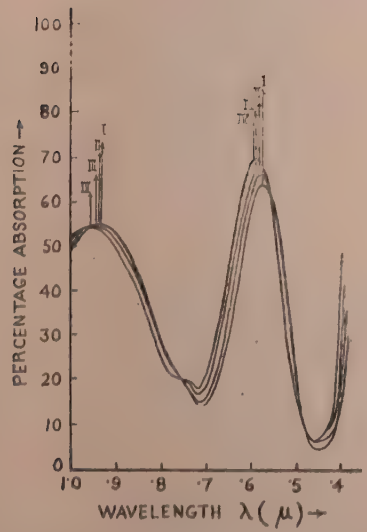

Fig. 15. Absorption curve of 3% $Ni(CH_3COO)_2$ solution

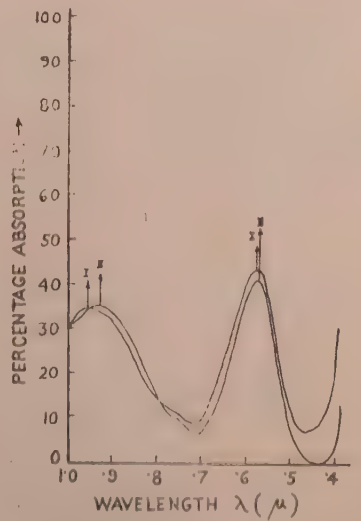

Fig. 16. Absorption curve of 2.25% $[Ni(NH_3)_4](SO_4)$

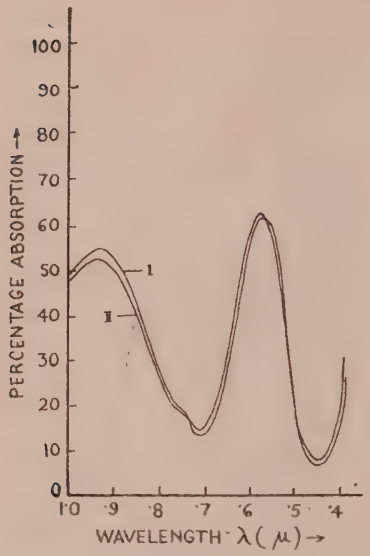

Fig. 17. Absorption curve of 1.5 % $[Ni(NH_3)_4]\ (OH)_2$ solution

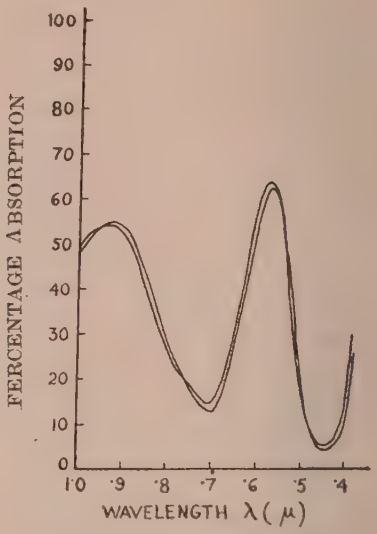

Fig. 18. Absorption curve of 2% $[Ni(NH_3)_4]\ (Cl)_2$ solution

DISCUSSION

(*a*) *The absorption spectra :*

For all the salt solutions studied in Table Ia, the absorption spectra consist of three maxima at about 13,900 cm^{-1}, 15,200 cm^{-1} and 25,350 cm^{-1} within the range of our studies. We shall designate them by II, III and IV respectively. The first maximum observed by Dreisch *et al.* (1937, 1939), which lies in the infra-red region for all the salts ($\sim$8500 cm^{-1}) except amino-salts (Table Ib, for which it lies in the visible range 10,800 cm^{-1}) will be known as I.

The maximum at about 15,370 cm^{-1} was detected by Dreisch and Trommer (1937) and was later identified by Owen (1955) as arising due to the transition from Stark-level Γ_2 to Γ_4 (Fig. 19). This is almost identical with our III. The maximum II was not detected by them but has recently been observed by Owen, Holmes and McClure (1957) in $NiSO_4.7H_2O$, $NiSiF_6.6H_2O$ and $K_2(Zn.Ni)(SO_4)_2.6H_2O$ (1% Ni) crystals and also in state of dilute aqueous solution of nickel sulphate using a spectrophotometer. The bands II and III were named as 'red band' by them. Hartmann and Müller (1958) using three glass prism spectrograph and infra-red sensitized plates found this 'red band' to be single. But on enlargement of the photographs this band showed a fine structure (four peaks named by them as *C*, *D*, *E* and *a*). Three of them are of almost equal intensity, while

the fourth one is very feeble. They then interpreted some of these structures in the light of the theory put forward by Hartmann (1954) and Furlanie (1957). They attributed the first two peaks (*C* and *D*) as due to tetragonal splitting, while the fourth peak (a) was assigned to the transition due to mixing but failed to account for the third peak (*E*) on the basis of the energy level diagram derived from ligand field splittings. According to Jörgensen (1958) also the occurrence of the peak (*E*) is a very puzzling problem. The assignment of Hartmann and Müller can not be correct for reasons to follow.

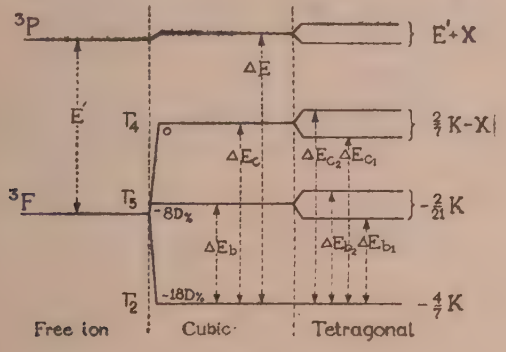

Fig. 19.

This third peak can not be due to vibrational level because then it would have been much affected by solvent, solute and dilution (Freed, 1942) and also this separation ($\sim$1300 cm^{-1}) is too high (Schultz, 1957). The intensity of this band is almost equal to the transitions from other Stark-levels and hence can not be also due to mixing (Orgel, 1955). According to Balhausen (1955) the occurrence of II and III bands is either due to tetragonal field effects or to (L, S) coupling effects. Jörgensen (1955) has pointed out that (L, S) coupling alone can not explain the occurrence of these bands.

b) *The crystal field and energy levels*

The ground state of Ni^{++} ion ($3d^8$ ^3F) under the influence of a crystalline electric field conforming to a potential of the type,

$$V = K' \left(x^4 + y^4 + z^4 - \frac{3}{5} r^4 \right) - T'_2(2z^2 - x^2 - y^2) + T'_4 \left(z^4 - 6x^2y^2 - \frac{3}{5} r^4 \right), \quad \ldots \quad (1)$$

where $K = \frac{2}{5} er^4 K'$, $T'_2 = er^2 T_2$, $T_4 = er^4 T'_4$ and $\bar{r}^4$ is the average value for the radius of $3d$-electrons, splits energy levels as shown in Fig. 19.

The so split levels will be approximately, taking the lowest as zero, given by (Owen, 1955)

$$
\left.\begin{array}{ll}
{}^3P & \left\{\begin{array}{ll} p_1 & E'+X+\frac{4}{7}K+\frac{4}{5}T_2-\frac{16}{105}T_4 \\ p_2 & E'+X+\frac{4}{7}K-\frac{2}{5}T_2-\frac{16}{105}T_4 \end{array}\right. \\
{}^3F & \left\{\begin{array}{ll} C_2 & \frac{6}{7}K-X+\frac{4}{35}T_2-\frac{44}{105}T_4 \\ C_1 & \frac{6}{7}K-X-\frac{8}{35}T_2-\frac{4}{105}T_4 \\ b_2 & \frac{10}{21}K+\frac{10}{105}T_4 \\ b_1 & \frac{10}{21}K-\frac{60}{105}T_4 \\ a & 0 \end{array}\right.
\end{array}\right\} \quad \ldots (2)
$$

From the experimental observations of Owen, Holmes and McClure (1957) on single crystals of $NiSO_4 . 7H_20$, (Zn, Ni) $.K_2(SO_4)_2.6H_2O$ and $NiSiF_6.6H_2O$ and on aqueous solution of $NiSO_4$, it is seen that $\Delta E_p \approx 3\Delta E_{b_2}$ (Fig. 19). This will be evident from the Table II., and hence $\left(\frac{10}{105}T_4\right)$ is very very small compared to ΔE_p. It is seen also that we are more correct if we take $\Delta E_p \approx 3\Delta E_b$.

TABLE II

Crystals	$\Delta E_{b_2}=\frac{10}{21}K+\frac{10}{105}T_4$ in cm^{-1}	ΔE_p in cm^{-1}	$3\Delta E_{b_2}-\Delta E_p=\frac{10}{105}T_4$ in cm^{-1}
$NiSO_4.7H_2O$	8600	25,500	300
$K_2.(Zn, Ni).(SO_4)_2.6H_2O$	8550	25,500	150
$NiSiF_6.6H_6O$	8550	25,500	150
$NiSO_4$(soln)	8500	25,300	200

Let us assign the band I due to transition $\frac{10}{21}K + \frac{10}{105}T_4 \rightarrow 0$ and call it as ΔE_{b_2}. Then

$$\Delta E_b = \frac{10}{21}K = \frac{1}{3}\Delta E_p$$

and hence

$$\Delta E_{b_2} - \Delta E_b = \frac{10}{105}T_4 \qquad \ldots (3)$$

From the expression (3) the value of T_4 can be calculated which comes out of the right order as suggested by Owen (1955). This also supports our argument that we are correct to take $\Delta E_p = 3\Delta E_b$.

Let us assign the other two bands II and III as due to transitions

$$C_1 \rightarrow 0$$

(as given by Eq. 2)

$$C_2 \rightarrow 0$$

and designate them by ΔE_{c_1} and ΔE_{c_2} respectively (Fig. 19); then following Owen, Holmes and McClure (1957) the band III can be taken as ΔE_c i.e.

$$\Delta E_{c_2} \approx \Delta E_c = \frac{6}{7}K - X \qquad \ldots (4)$$

if the effect of T_2 and T_4 are neglected (in this we are justified as T_2 and T_4 are themselves small and are of opposite sign in the expression for energy). From expression (4) X comes out as 100 cm^{-1}. This X may be neglected compared to $\frac{6}{7}K$ while fitting the optical data. Hence we get

$$\Delta E_p = 3\Delta E_b = \frac{10}{7}K = \frac{5}{3}\Delta E_c \qquad \ldots (5)$$

So from a measurement of either of ΔE_p or ΔE_b or ΔE_c one can evaluate K which are shown in Table III.

In nickel-amino-salts K is calculated directly without any approximation since the transition ΔE_b is known.

K-values (Table III) indicate that in state of solution all the six members of the cluster about the Ni^{++} ion may be the same in Tutton-salts and halides etc. but in amino-salts they will be different.

c) *Evaluation of the term separation* (E')

For ions where ^3F-term lies lowest, the term separation E' in crystals, which is an important spectroscopic constant, can be evaluated if at least two out of the three transitions are observed (Owen, 1955). From Fig. 1 it is seen that

$$E' = \Delta E_p + \Delta E_c - 3\Delta E_b \quad \ldots (6)$$

(neglecting the small tetragonal terms)

From which we have

$$E' = \Delta E_c \quad \text{(a very good approximation)} \quad \ldots (7)$$

In amino-salts E' can be evaluated without any approximation however small they might be since all the three transitions have been observed. These are given in Table III.

TABLE III

salts	K-values cm^{-1}	E'-values cm^{-1}	f-values	μ-values (soln.) at 300°K		g-values at 300°K	
				Optical	Magnetic	Calculated	Observed
$NiSO_4$	17,725	15,200	0.900	3.278	3.319	2.280	2.20*
$NiSeO_4$	17,725	15,220	0.901	3.278	3.258	2.280	
$Ni(NH_4.SO_4)_2$	17,745	15,240	0.902	3.277	3.219	2.277	2.25**
$Ni(K.SO_4)_2$	17,745	15,220	0.901	3.277	3.314	2.277	2.25**
$Ni(Rb.SO_4)_2$	17,725	15,150	0.896	3.268	..	2.276	
$Ni(Tl.SO_4)_2$	17,745	15,240	0.902	3.277	3.321	2.277	2.25**
$Ni(NH_4SeO_4)_2$	17,725	15,200	0.900	3.278	3.184	2.280	
$Ni(K.SeO_4)_2$	17,725	15,200	0.900	3.278	3.193	2.280	
$NiCl_2$	17,725	15,270	0.904	3.278	3.245	2.280	2.21***
$NiBr_2$	17,725	15,200	0.900	3.277	3.286	2.280	
$Ni(NO_3)_2$	17,725	15,220	0.901	3.278	3.326	2.280	
$Ni_3Bi_2(NO_3)_{12}$	17,745	15,150	0.896	3.277		2.280	
$Ni(CHOO)_2$	17,725	15,150	0.896	3.268		2.276	
$Ni(CH_3COO)_2$	17,725	15,200	0.900	3.278	3.322	2.280	
$Ni[(NH_3)_4](SO_4)$	22,115	13,470	0.797				
$Ni[(NH_3)_4](OH)$	22,030	13,620	0.805				
$Ni[(NH_3)_4](Cl)$	22,470	13,070	0.773				
$Ni[(NH_3)_4](CH_3COO)$	22,512	13,010	0.770				

* Ono (1953) ** Griffiths and Owen (1952) *** Ting and Williams (1951)

It is observed that there is a lowering of the term separation E' for Ni^{++} ion in crystal from the free ion value of $E = 16{,}900\ cm^{-1}$ (Moore, 1952).

Following Owen (1955) this lowering may be attributed to the covalency factor f^2 arising from partial overlap of the 3*d*-orbitals with σ- and π-orbitals of the surrounding atoms.

Hence
$$\frac{E'}{E} = f^2 \qquad \ldots (8)$$

where $f^2 = f_\sigma^2 \cdot f_\pi^2$.

In ordinary nickel salts f_π^2 is unity. From the above relation one can calculate f^2 which are given in Table III.

Primarily this covalency factor should not be different for all the salts in which Ni^{++} ion is similarly coordinated with six water molecules, but there might be appreciable change in the overlap between Ni^{++} ion and that of oxygen and hence in the covalency factor from salt to salt arising from the effect of distant atoms. In state of solution distant atom effect will be negligible and hence covalency factor should not vary appreciably from salt to salt with similar coordination.

An examination of the f^2-values shows that in all the nickel salts $f^2 \approx 0.9$ except for the amino-salts, where it tends to be 0.78. This suggests that f_π^2 may not be negligible in nickel amino-salts. As a result both σ-and π-orbital overlap may exist, so that $f_\pi^2 \approx 0.9$ and $f_\sigma^2 \approx 0.85$ making $f^2 = 0.76$ nearly as observed.

d) Evaluation of the mean magnetic moment μ

Following Schlapp and Penney (1932), Griffiths and Owen (1952) the principal magnetic moments $\mu_\parallel$ and $\mu_\perp$ along and normal to the axis of symmetry of the water cluster about the Ni^{++} ion are given by

$$\left.\begin{aligned} \mu^2_\parallel &= 8\left[\left\{1+8\lambda\alpha'_\parallel + \frac{\theta_\parallel}{kT} + \ldots\right\} - 3kT\alpha'_\parallel\right] \\ \mu^2_\perp &= 8\left[\left\{1+8\lambda\alpha'_\perp + \frac{\theta_\perp}{kT} + \ldots\right\} - 3kT\alpha'_\perp\right] \end{aligned}\right\} \qquad \ldots (9)$$

where $\theta_\parallel = 4/3\lambda^2 \cdot (\alpha'_\perp - \alpha'_\parallel)$ and $\theta_\perp = 2/3\lambda^2 \cdot (\alpha'_\parallel - \alpha'_\perp)$, λ is the spin-orbit coupling constant for the free ion and is equal to $-324\ cm^{-1}$ (Shenstone and Willets 1951), $\alpha'_\parallel$ and $\alpha'_\perp$ are the coefficients of the crystal field.

From the relation (9)

$$\mu^2 = \frac{\mu^2_\parallel + 2\mu_\perp^2}{3} = 8\{1+(8\lambda - 3kT)\alpha'\} \qquad \ldots (10)$$

where $$\alpha' = \frac{\alpha'_{\parallel} + 2\alpha'_{\perp}}{3} = \frac{f^2}{\Delta E_b} = -2.1\frac{f^2}{K}.$$

Hence utilising our K-values and f^2-values μ for Ni^{++} ion in different salts in state of solution are evaluated and given in Table IV. In order to check these deduced values we have measured the magnetic susceptibilities of nickel salts in state of aqueous solution at concentrations of optical measurements by modified Curie balance (unpublished, D.Neogy). These are also given in Table IV. There is a close agreement between these two sets of values.

(*e*) *Calculation of the splitting factor 'g' :*

According to Owen (1955) the splitting factor for Ni^{++} ion is given by the relation

$$g = 2 - \frac{128\lambda}{K} \cdot f^2 \qquad \ldots (11)$$

where the symbols have their usual meaning.

Thus one can calculate g-values in state of solution from the optically observed K and f^2-values. These are given in Table IV. Directly measured g-values in state of solution are not available for comparison. However, it is interesting to note that g-values for some of the nickel salts in crystalline state do not differ much from our evaluated values.

(*f*) *Anisotropy of the cluster about the Ni^{++} ion in state of solution:*

For the octahedrally coordinated Ni^{++} ion, in the salts studied the predominent cubic component of crystalline electric field acting upon it from the surrounding charges splits its original J-multiplet state $3d^8\ ^3F$ into an orbital singlet lying at about 10^4 cm^{-1} below the two triplets. A very small rhombic component of the field removes the orbital degeneracy of the triplets. Van Vleck (1932), Schlapp and Penney (1932), Griffiths and Owen (1952), Bleaney and Stevens (1953) and Stevens (1953) have calculated the three principal susceptibilities under the above conditions. Bose *et al.* (1958) have shown that on the assumption of an approximate tetragonal symmetry and since in nickel salts $K_\perp$, susceptibility normal to the tetragonal axis is greater than $K_\parallel$ that along the tetragonal axis, the anisotropy of the individual paramagnetic unit is given by

$$\left.\begin{aligned} \Delta K = K_\perp - K_\parallel &= \frac{8N\beta^2}{3kT}\left\{8\lambda - 3kT - \frac{2\lambda^2}{kT} + G\right\} \times (\alpha_\perp - \alpha_\parallel) f^2 \\ \text{where} \quad G &= 16\lambda^2 (\alpha_\perp + \alpha_\parallel) f^2 + \frac{2\lambda}{3kT}\left[(\alpha_\perp + 2\alpha_\parallel) f^2 + 2\lambda \{\alpha_\perp^2 + 2\alpha_\parallel^2\} f^4\right] \end{aligned}\right\} \quad \ldots (12)$$

and $\alpha_\perp$ and $\alpha_\parallel$ are the principal field coefficients related to the splittings of the orbital levels in a tetragonal field.

$\alpha_\perp$ and $\alpha_\parallel$ must be known from optical observations before one can calculate ΔK. This is done in the following manner :

As shown in Fig. 20 the split levels in a tetragonal field are named as ΔE_{e2}, ΔE_{c2}, ΔE_{c1}, ΔE_{b2} and ΔE_{b1}. Then we will have

$$-\frac{1}{\alpha_\parallel''} = \Delta E_{c2} \quad \text{and} \quad -\frac{1}{\alpha_\perp''} = \Delta E_{c1}$$

further $$-\frac{1}{\alpha_\parallel} = \Delta E_{b2} \quad \text{and} \quad -\frac{1}{\alpha_\perp} = \Delta E_{b1} \qquad \ldots \quad (13)$$

When the tetragonal components are absent the mean centres are ΔE_c and ΔE_b which are related as

$$\Delta E_c = 1.8\, \Delta E_b \qquad \ldots \quad (14)$$

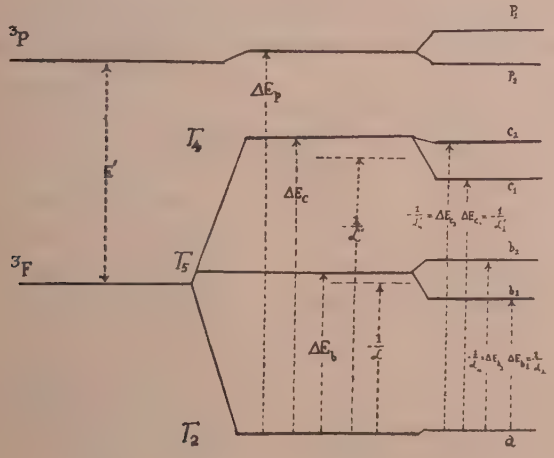

Fig 20. The effect of tetragonal field on α and α''.

The effect of the tetragonal field is to make the mean centres as $-\frac{1}{\alpha''}$ and $-\frac{1}{\alpha}$, where

$$\alpha'' = \frac{\alpha_\parallel'' + 2\alpha_\perp''}{3}, \quad \alpha = \frac{\alpha_\parallel + 2\alpha_\perp}{3}$$

and $$\alpha = 1.8\alpha''$$

Since we have observed ΔE_{c2} and ΔE_{c1}, hence α'' can be calculated.

From the expression (2) it can be seen that

$$\alpha = 1.8\alpha'' = \frac{1}{3}\left[\frac{1}{A+B} + \frac{2}{A-6B}\right]$$

where $A = \frac{10}{21} K$ and $B = \frac{10}{105} T_4$

Thus the value of T_4 for different salts can be evaluated. These are included in Table IV. Hence using the values of K and T_4 for different salts in Eq. (13) $\alpha_\perp$ and $\alpha_\parallel$ are immediately obtained and from which ΔK. These values are shown in Table IV.

We have included ΔK-values so calculated in Table IV and for comparison given the ΔK-values from magnetic measurements by Bose *et al.* (1958). The difference that is observed between the anisotropies of the paramagnetic unit in state of aqueous solution and in crystalline state can be well understood follow-

TABLE IV

Salts	T_4	$-\alpha_\perp \times 10^5$	$-\alpha_\parallel \times 10^5$	$\Delta K \times 10^5$ Optical	$\Delta K \times 10^5$ Magnetic
		(a) Sulphate Series			
Heptahydrate	1315	13.005	11.675	204	258
NH_4	1315	13.007	11.675	204.8	210*
K	1351	13.987	11.666	204	261.7
Rb	1430	13.123	11.660	223	280.1
Tl	1365	13.038	11.654	211.8	221.1
		(b) Selonate Series			
Hexahydrate	1386	13.072	11.665	215.3	370
NH_4	1339	13.029	11.671	208	212**
K	1339	13.029	11.671	208	234.5
		(c) Halide Series			
Cl_2	1290	12.987	11.679	201	
Br_2	1315	13.012	11.665	212	
		(d) Nitrate Series			
(NO_3)	1315	13.005	11.675	204	
Bi	1733	13.405	11.609	274	
		(e) Organic Base Series			
(CHOO)	1430	13.123	11.660	223	
$(CH_3\ COO)$	1315	13.005	11.675	204	370***

* Krishnan *et al.* (1933.) ** Mookherji (1946.) *** Mathur (unpublished)

ing Van Vleck (1939), Bose *et al.* (1958) and Bose and Mitra (1952). According to them the major cubic field arises from the water cluster about the Ni^{++} ion in the hydrated salts and hence leaves an orbital singlet lowest in the Stark-pattern. The primary Jahn-Teller effect can very feebly distort the water cluster resulting in the feeble anisotropy of the electric field about the Ni^{++} ion. In order to explain 5% to 8% anisotropy of the cluster there must be an additional distortion of the $[Ni(H_2O)_6]^{++}$ cluster. This is supplied by the field of charges or dipoles outside the cluster i.e. by the effect of the distant atoms. Now in state of solution this effect of distant atoms will be very small and hence the additional distortion. As a result magnetic anisotropy ΔK of $[Ni(H_2O)_6]^{++}$ cluster in state of solution should differ from that of crystalline state. It is observed that this distant atom effect is very much pronounced in the double sulphates and selenates of *K*, *Rb* and single sulphate and not so much pronounced in double sulphates and selenates of NH_4 and Tl.

We have made measurements with a single crystal of $Ni.K_2(SO_4)_2.6H_2O$. The observed bands are at 14,145 cm^{-1}, 15,550 cm^{-1} and 26,000 cm^{-1}. The calculated value of K is 18,197 cm^{-1}, E' is 15,550 cm^{-1} and hence $f^2 = 0.92$. Taking this f^2 value and K we have calculated μ, g and ΔK values. These are as follows :

	Calculated	Observed
μ	3.27	3.18
g	2.28	2.25
ΔK	240	261.4

The agreement between the observed values and calculated values is very good.

If one accepts the findings of Hartmann and Muller (1958) that the tetragonal splitting in $NiSO_4.7H_2O$ and $NiSO_4.6H_2O$ crystals is $\sim$400 cm^{-1} as correct and calculate ΔK then one gets a very absurd value of ΔK. For heptahydrate ΔK comes out as 530×10^{-6} as against 254 (magnetic measurements) and for hexahydrate the same value as against 354 (magnetic measurements). Thus the findings of Hartmann and Müller can not be correct.

ACKNOWLEDGMENTS

The work was carried out at the Physics Laboratories of Agra College, Agra. We wish to express our sincere thanks to University Grants Commission due to whose generous grant it was possible to purchase the 'Uvispek' spectrophotometer which enabled us to carry out this piece of work.

Our sincere thanks are also due to Professor A. Bose, D.Sc., F.N.I., for his helpful criticisms and concrete suggestions.

REFERENCES

Bethe, H., 1929, *An. Physik*, **8**, 133.
Bethe, H., 1930, *Z. Physik*, **60**, 218.
Bleaney, B. and Stevense, K. W. H., 1953, *Rep. Progr. Phys.*, **16**, 108.
Bose, A. and Mitra, S. K., 1952, *Ind. Jour. Phys.*, **26**, 393.
Bose, A., Mitra, S. K. and Datta, S. K., 1958, *Proc. Roy. Soc.*, *A***248**, 153.
Ballhaussen, 1955, C. J. Kgl. Danske Vindenskab., Selskab, Mat. fgs. Medd. No. 8, 29.
Dreisch, Th.and Trommer, W., 1937, *Z. Phys. Chem.*, *B* **37**, 40.
Dreisch, Th. and Kallscheuer, O., 1939, *Z. Phys. Chem.*, *B* **45**, 19.
Freed, S., 1942, *Rev. Mod. Phys.*, **14**, **105**,
Furlanei, 1957, *Z. Physik Chem.*, **10**, 291.
Gorter, C. J., 1932, *Phys. Rev.*, **42**, 437.
Griffiths, J. H. and Owen, J., 1952, *Proc. Roy. Soc.*, *A***213**, 451.
Hartmann, H., 1954, Theorie der chemschen Bindung auf quantentheoretischer Grendlage. Springer verlag.
Hartmann, H. and Muller, 1958, *Discussions of Farad., Soc.*, **26**, 49.
Jorgensen, CHR. Klixbull, 1955, *Acta. Chem. Scand.*, **9**, 1362.
„ 1958, *Discussions of Farad. Soc.*, **26**, 90.
Krishnan, K. S., Chakravorty, N. C. and Banerjee, S., 1933, *Philos. Trans.*, **232**, 99.
Mookherji, A., 1946, *Ind. Jour. Phys.*, **20**, 9.
Mookherji, A. and Chhonkar, N. S., 1959, *Ind. Jour. Phys.* **42**, 74.
Moore, C. E., 1952, Atomic Energy Levels—Nat. Bur. Stand. circ. 467, Vol. II.
Orgel, L. E., 1955, *J. Chem. Phys.*, **23**, 1004.
Owen, J., 1955, *Proc. Roy. Soc.*, **227**, 183.
Owen, G. Holmes and Donald S. McClure, 1957, *J. Chem. Phys.*, **26**, 1686
Ono, 1953, *J. Phys. Soc. Japan*, **8**, 802.
Polder, D., 1942, *Physika*, **9**, 709.
Schlapp, R. and Penney, W. G., 1932, *Phys. Rev.*, **42**, 1666.
Schultz, M. L., 1942, *J. Chem. Phys.*, **10**, 194.
Stevense, K. W. H., 1953, *Proc. Roy. Soc.*, *A***219**, 542.
Schenstone and Willets, 1951, *Phys. Rev.*, **41**, 208.
Ting and Williams, 1951, *Phys. Rev.*, **82**, 507.
Van Vleck, J. H., 1932, *Phys. Rev.*, **41**, 208.
Van Vleck, J. H., 1939, *J. Chem. Phys.*, **61**, 72.

ON THE ELECTRONIC SPECTRA OF 2-BROMO-AND 3-BROMOPYRIDINE IN DIFFERENT STATES AND IN SOLUTIONS

T. N. MISRA

Optics Department, Indian Association for the Cultivation of Science, Calcutta 32.

(*Received, May* 30, 1960)

ABSTRACT. The ultraviolet absorption spectra of 2-bromo- and 3-bromopyridine in all the three phases and also of their solutions have been investigated and a tentative assignment of the bands of the vapours has been made.

In the vapour phase, 3-bromopyridine exhibits two systems of discrete bands, one due to the $n \rightarrow \pi^*$ transition (Transition I) and the other due to $\pi \rightarrow \pi^*$ transition (Transition II). In the liquid state, in the solid state at −180°C and in solution in alcohol, the $n \rightarrow \pi^*$ transition is absent and only one system of bands due to $\pi \rightarrow \pi^*$ transition is observed. In the spectrum due to the solution in 3-methyl pentane, however, the $n \rightarrow \pi^*$ transition persists. It is suggested that the molecules of 3-bromopyridine form associated groups through the nitrogen sp^2 electron and the hydrogen atom of neighbouring molecules in the states of aggregation of the pure substance.

In the case of 2-bromopyridine it is confirmed that the $n \rightarrow \pi^*$ transition is absent not only in the state of aggregation and in solution in alcohol but also in its spectra due to the vapour phase and solution in 3-methyl pentane probably due to the intramolecular inductive influence of the bromine atom on the sp^2 electron of the adjacent nitrogen atom as suggested by earlier workers.

INTRODUCTION

It is now an established fact (Kasha, 1950; Rush and Sponer, 1952) that in the near ultraviolet absorption spectrum of *N*-hetrocyclic compounds in the vapour state there is a second system of bands due to the excitation of a nonbonding sp^2 electron of the nitrogen atom to the first unfilled π-molecular orbital of the ring called $n \rightarrow \pi^*$ transition besides the system due to $\pi \rightarrow \pi^*$ transition.

Recently, Banerjee (1956, 1957) studied the absorption spectra of pyridine and the three isomeric picolines in the liquid state and in the solid state at low temperature and observed that the second system of bands due to the $n \rightarrow \pi^*$ transition disappears with liquefaction of the vapour and it is absent also in the spectrum due to the substances in the solid state. The absence of the $n \rightarrow \pi^*$ transition in the liquid and solid states was explained by him on the assumption that in these states of aggreegation the molecules are associated through weak

virtual bonds formed by the non-bonding electron of the nitrogen atom and the hydrogen atom of neighbouring molecules.

Roy (1958) studied the absorption spectra of solutions of pyridine in different solvents and obtained both $n \rightarrow \pi^*$ and $\pi \rightarrow \pi^*$ transitions in solutions in cyclohexane, 3-methyl pentane and carbon tetrachloride. But in the spectrum due to the solution in isobutyl alcohol, the $n \rightarrow \pi^*$ transition was found to be absent and this was attributed to the formation of a bond between the pyridine molecule and the OH group of alcohol molecule through the non-bonding electron of the nitrogen atom.

Stephenson (1954) studied the absorption spectra of some substituted pyridine compounds including 2-bromopyridine and 3-bromopyridine dissolved in iso-octane and ethyl alcohol. In the case of solution of 3-bromopyridine in ethyl alcohol the $n \rightarrow \pi^*$ transition was found to be absent, but it appeared in the spectrum due to the solution in iso-octane. In the case of 2-bromopyridine, however, no change in intensity was observed in the low energy region when the solvent was changed from iso-octane to alcohol. The $n \rightarrow \pi^*$ transition was found to be absent also in the spectrum due to vapour of this substance. He concluded from these results that the $n \rightarrow \pi^*$ transition was absent in the spectrum due to 2-bromopyridine. He explained this absence of the $n \rightarrow \pi^*$ transition on the assumption that inductive attraction of halogen atom attached to the adjacent carbon atom increases the binding energy of the nonbonding electrons of the nitrogen atom and consequently the bands due to the $n \rightarrow \pi^*$ transition are shifted to the region of the bands due to $\pi \rightarrow \pi^*$ transition.

The present work was undertaken to investigate the ultraviolet absorption spectra of 2-bromo- and 3-bromopyridine in the vapour state and to analyse the bands, if possible, because Stephenson (1954) had not analysed these bands. It was also intended to find out whether the $n \rightarrow \pi^*$ transition is actually absent in the case of 2-bromopyridine in the vapour state.

The absorption spectra of these compounds in the solid and liquid states and in solutions in different solvents have also been studied in order to compare these spectra with those due to the substances in the vapour state.

EXPERIMENTAL

Chemically pure samples of 2-bromo- and 3-bromopyridine supplied by Fluka, Switzerland, were fractionated and the proper fractions were distilled under reduced pressure before use. To study the spectra due to the vapour absorption, cells of length 50 cm and 10 cm were used. The cell was filled up with the vapour at saturation vapour pressure at different temperatures and the spectra due to the vapour at different densities were photographed. Two separate electrical heaters, one for the absorption cell and the other for the bulb containing the liquid and

attached to the absorption cell, were used to control the temperature. The reservoir containing the liquid was always kept at a temperature about 5°C lower than that at any part of the absorption cell. To produce a low pressure in the vapour in the absorption tube, the tube was kept at the room temperature while the bulb containing the liquid was immersed in a suitable low temperature bath.

To record the bands due to $\pi \rightarrow \pi^*$ transition in 3-bromopyridine, the 10 cm cell was used and it was kept at the room temperature while the reservoir was kept at 0°C. The 50-cm cell under similar conditions was used to record the bands due to the $n \rightarrow \pi^*$ transition. In the case of 2-bromopyridine an absorption cell of length 50 cm was used and the reservoir was kept at 0°C for studying the $\pi \rightarrow \pi^*$ transition and at 50°C for studying $n \rightarrow \pi^*$ transition.

Very thin films of thickness of the order of a few microns of the substances in the liquid and solid states were required to produce absorption bands due to $\pi \rightarrow \pi^*$ transition. Thicker films of the liquids were also used to find out whether bands corresponding to $n \rightarrow \pi^*$ transition were present.

The solvents used to study the absorption spectra of the substances in the solutions were ethyl alcohol and 3-methyl pentane. The solvents were found to produce no absorption band in the region under consideration. In this case, a brass cell 5mm thick provided with quartz windows was used and the strength of the solution was varied from .01% to .08% by weight. Spectrograms were taken on Agfa Isopan film with a Hilger E 1 spectrograph giving a dispersion of the order of 3 Å per mm. in the region of 2600 Å. Iron arc spectrum was taken on each spectrogram as a comparison.

Microphotometric records were taken with a Kipp and Zonen self-recoding microphotometer. The absorption spectra were calibrated with the help of microphotometric records of the iron lines using the method described in an earlier paper (Sirkar and Misra, 1959).

As the Raman and infrared spectra of these two substances had not been studied by previous workers, infrared absorption spectra of very thin films of the substances were recorded with a Perkin-Elmer Model 21 spectrophotometer using rock salt optics in order to find out the ground state vibrations and these were used to verify the excited state frequencies derived from the ultraviolet absorption spectra.

RESULTS AND DISCUSSION

Microphotometric records of the absorption spectra of 3-bromo- and 2-bromopyridine in different states and in solutions are reproduced in Figs. 1–6. The wave numbers of the bands in cm^{-1}, approximate intensities and their probable assignments are given in Tables I, II, III and IV.

3-*Bromopyridine*

(a) *Spectrum of the vapour phase.*

The absorption spectrum of 3-bromopyridine in the vapour phase (Fig. 1) shows two distinct systems of bands under different conditions of pressure and length of absorbing column of the the vapour. With the vapour at the saturation pressure at 4°C and with an absorption tube 50 cm long, a system of absorption bands starting at about 35000 cm ^{1} followed by region of complete absorption is observed. The bands of this system are sharp and narrow and following Kasha (1950), they have been attributed to the $n \rightarrow \pi^*$ transition (Transition I). At lower pressure of the vapour in a shorter cell, the second band system appears in the region 36000 cm^{-1} to 39000 cm^{-1} and the broad bands of this system resemble those due to other substituted benzenes arising from the $\pi \rightarrow \pi^*$ transition(Transition II). The analysis of the bands of these two systems is discussed separately in the following sections.

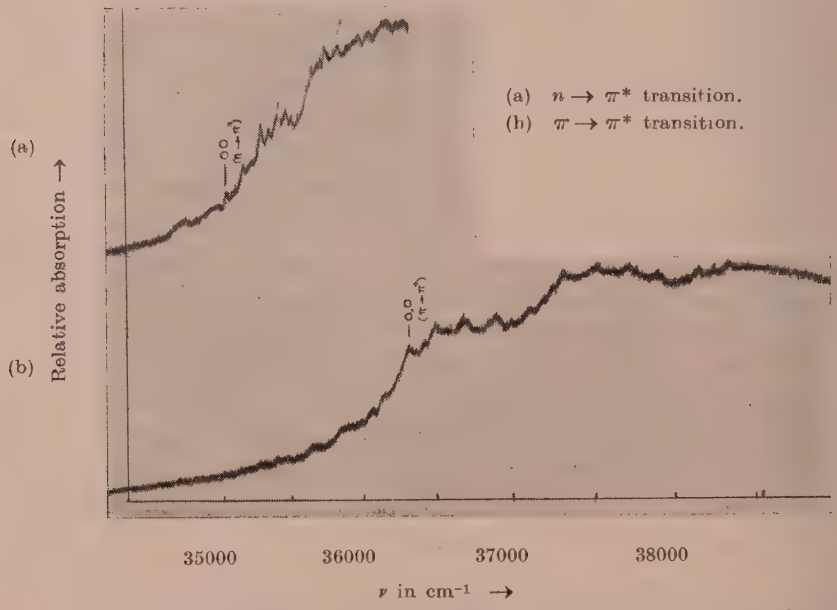

Fig. 1. Microphotometric records of the ultraviolet absorption spectra of 3-bromopyridine in the vapour state.

i) $\pi \rightarrow \pi^*$ *transition* (*Transition II*)

The strong band at 36300 cm^{-1} in this system has been taken as the 0, 0 band. Most of the remaining strong bands represent transitions involving excited state

TABLE I

Ultraviolet absorption bands of 3-bromopyridine in the vapour phase

Wave no. (cm^{-1}) and intensity	Assignment	Wage No. (cm^{-1}) and intensity	Assignment
Transition I ($n \rightarrow \pi^*$)		Transition II ($\pi \rightarrow \pi^*$)	
34778 (wb, diffuse)	?	35866 (mw)	0—434
34925 (wb, diffuse)	?	35986 (w)	0—314
35080 (w)	0, 0	36064 (mw)	0—236
35183 (s)	0+103	36123 (w)	0—177
35238 (w)	0+158	36300 (s)	0, 0
35310 (s)	0+230	36458 (s)	0+158
35359 (s)	0+279	36526 (w)	0+226
35412 (w)	0+103+230	36579 (w)	0+279
35429 (s)	0+349	36672 (s)	0+372
35469 (s)	0+158+230	36835 (w)	0+158+372
35517 (ms)	0+2×103+230	36875 (s)	0+575
35564 (ms)	0+2×103+279	36971 (w)	0+671
35621 (w)	0+2×158+230	37081 (m)	0+781
35659 (m)	0+579	37163 (m)	0+863
35702 (w)	0+158+2×230	37246 (m)	0+946
35752 (m)	0+2×103+2×230	37309 (s)	0+1009
35857 (s, b)	0+2×158+2×230 ($\pi \rightarrow \pi^*$?)	37532 (s)	0+372+863
35986 (ms, b)	0+2×279+349 ($\pi \rightarrow \pi^*$?)	37721 (s)	0+1421
36062 (ms, b)	0+2×349+279 ($\pi \rightarrow \pi^*$?)	37884 (s)	0+375+1009
		38171 (s)	0+863+1009
		38247 (m)	0+946+1009
		38324 (m)	0+2×1009

vibrational frequencies 158, 226, 279, 372, 575, 671, 781, 863, 946, 1009 and 1421 cm^{-1} and also ground state frequencies 177, 236, 314 and 430 cm^{-1} as shown in Table I. In order to find out the ground state vibrational frequencies, the infrared absorption spectrum of a very thin film of 3-bromopyridine with NaCl optics was studied. The wave numbers of the observed infrared bands are 695(s),

785(s), 870(vw), 1002(s), 1082(s), 1090(h)*, 1188(vw), 1319(vw), 1416(s), 1462(ms), 1558(h) and 1572(ms). The strength of the absorption at the bands are given in parentheses.

The infrared absorption bands at 695 cm^{-1}, 785 cm^{-1}, 870 cm^{-1}, 1002 cm^{-1} and 1082 cm^{-1} may be the ground state frequencies corresponding to the excited state frequencies 671 cm^{-1}, 781 cm^{-1}, 863 cm^{-1}, 946 cm^{-1} and 1009 cm^{-1} respectively. The absorption band apparently arising from the excited state frequency 1421 cm^{-1} may have actually been produced by two excited state vibrations, the corresponding ground state frequencies being 1416 cm^{-1} and 1462 cm^{-1} observed in the infrared and this may explain why this band is broader than the other bands.

The ground state values of the excited state frequencies 158 cm^{-1}, 226 cm^{-1}, 279 cm^{-1} and 372 cm^{-1} may probably be 177 cm^{-1}, 236 cm^{-1}, 314 cm^{-1} and 430 cm^{-1} respectively observed on the longer wavelength side of the 0, 0 band as $v \rightarrow 0$ transitions.

(*ii*) $n \rightarrow \pi^*$ *transition* (*Transition I*)

The $n \rightarrow \pi^*$ transition of 3-bromopyridine lies in the region 35000 cm^{-1} to 36000 cm^{-1}. Assuming the band at 35080 cm^{-1} as the 0, 0 band of this system, the other bands can be assigned as progression of frequencies 103, 158, 230, 279, 349 and 579 cm^{-1} and their combinations as shown in Table I. The bands at 35857 cm^{-1}, 35986 cm^{-1} and 36062 cm^{-1} are not narrow line-like bands unlike the other bands of this system. The high intensity and large breadth of these bands may be due to superposition of bands due to $n \rightarrow \pi^*$ on the bands of the $\pi \rightarrow \pi^*$ transition. Thus the band at 35857 cm^{-1} may be assigned as an $n \rightarrow \pi^*$ transition $(0 + 2 \times 158 + 2 \times 230)$ superimposed on the $(0 - 434)$ band of the $\pi \rightarrow \pi^*$ transition. Similarly, the other two bands are formed by superposition of the bands $(0 + 2 \times 279 + 349)$ and $(0 + 2 \times 349 + 279)$ of $n \rightarrow \pi^*$ system on the bands (0—314) and (0-236) of the $\pi \rightarrow \pi^*$ system respectively.

No attempt has been made to assign the two broad diffuse bands at 34778 cm^{-1} and 34925 cm^{-1} since they have structures entirely different from those of bands due to both $n \rightarrow \pi^*$ and $\pi \rightarrow \pi^*$ transitions.

(*b*) *Spectra of the solutions*

In the spectrum of .01% solution of 3-bromopyridine in ethyl alcohol (Fig. 2) only three broad bands are observed in the region 36000 cm^{-1} to 38000 cm^{-1}, the 0,0 band being assumed to be at 36197 cm^{-1}. The other two bands form progression of excited state frequency 966 cm^{-1} and its harmonics. The nature and position of these bands suggest that they belong to the $\pi \rightarrow \pi^*$ system. With increased concentration, the long wavelength side was photographed, but no

* 'h' indicates a hump in the absorption curve.

band system corresponding to the $n \rightarrow \pi^*$ transition observed in the vapour could be detected.

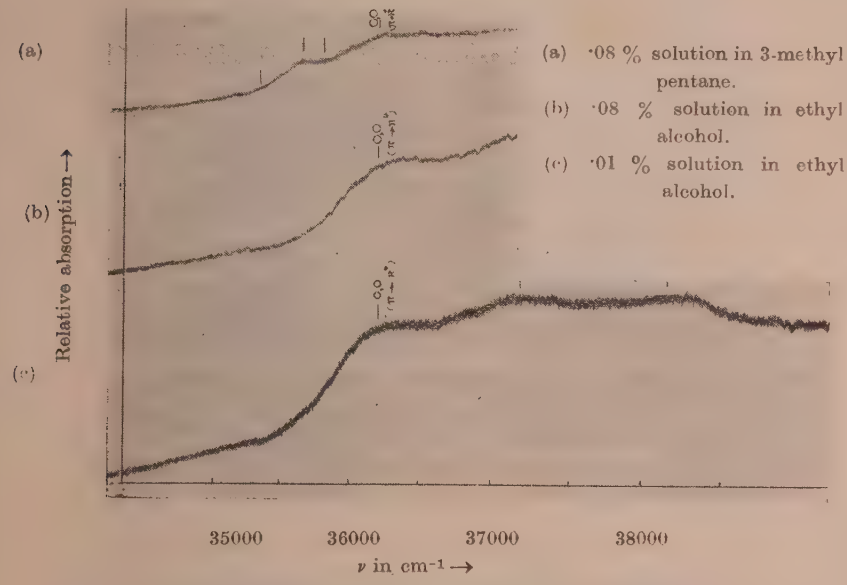

Fig. 2. Microphotometric records of the ultraviolet absorption spectra of solutions of 3-bromopyridine

In the spectrum due to the solution in 3-methyl pentane a broad band extending from 35327 cm^{-1} to 35806 cm^{-1} with the peak at 35650 cm^{-1} was observed which probably corresponds to the $n \rightarrow \pi^*$ transition. The structure was, however, not resolved. The result is in agreement with that reported by Roy (1958) who observed the $n \rightarrow \pi^*$ transition in solution of pyridine in 3-methyl pentane and it was found to be absent in the solution in isobutyl alcohol. This absence of $n \rightarrow \pi^*$ transition in solution in alcohol was explained by Stephenson (1954) and Roy (1958) by assuming that in the solution in alcohol, the non-bonding sp^2 electrons of the nitrogen atom become involved in formation of a hydrogen bond while in the solution in 3-methyl pentane no such bond-formation takes place.

(*c*) *Spectra in the solid and liquid states*

Both in the liquid and solid states (Fig. 3a and 3b) only one system of borad bands corresponding to the $\pi \rightarrow \pi^*$ transition is produced by this substance and the system due to $n \rightarrow \pi^*$ transition did not appear even when a thick film was used as the absorber.

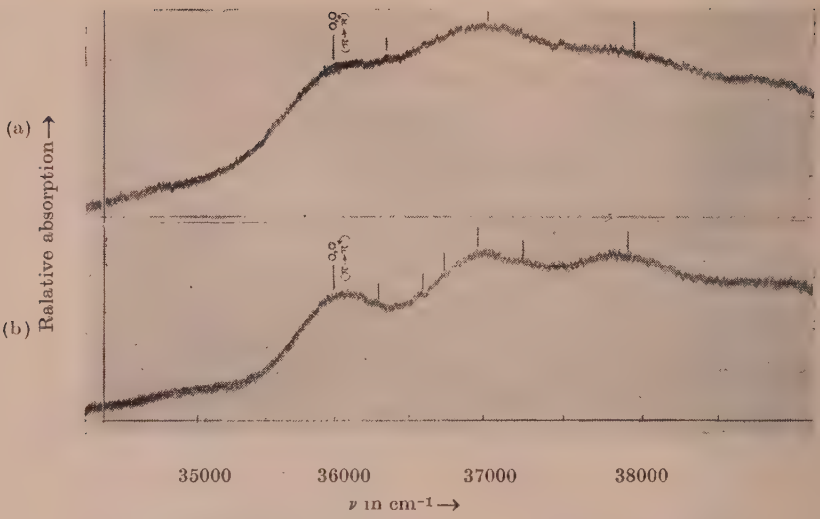

Fig. 3. Microphotometric records of the ultraviolet absorption spectra of 3-bromopyridine
(a) Liquid at 32°C. (b) Solid at —180°C.

TABLE II

Ultraviolet absorption bands of 3-bromopyridine

	Liquid at 32°C		Solid at –180°C		Solution at 32°C			
	Wave No. (cm^{-1}) and intensity	Assignment	Wave No. (cm^{-1}) and intensity	Assignment	Wave No. (cm^{-1}) and intensity	Assignment	Wave No. (cm^{-1}) and intensity	Assignment
Transition I					.08% sol. in alcohol		.08% sol. in 3-methyl pentane	
	Absent		Absent		Absent		Broad band extended from 35327 cm^{-1} to 35806 cm^{-1}	
Transition II					.01% sol in alcohol			
	35973 (s)	0, 0	35986 (s)	0, 0	36197 (s)	0, 0		
			36268 (w)	0+282				
	36329 (m)	0+356	36570 (mw)	0+584				
			36713 (m)	0+727				
	36943 (s)	0+970	36951 (s)	0+965	37163 (s)	0+966		
			37247 (m)	0+1261				
	37913 (s)	0+2×970	37920 (ms)	0+2×965	38134 (s)	0+2×966		

In the spectrum due to the liquid the 0, 0 band has been identified with that at 35973 cm^{-1} and the other bands indicate a progression of vibrational frequencies 356 and 970 cm^{-1} in the excited state. The 0, 0 band of this system thus shifts by about 327 cm^{-1} towards red with the change from the vapour to the liquid state.

When the liquid is solidified and cooled to $-180°C$, the bands become sharper and assuming the 0,0 band to be at 35986 cm^{-1}, the spectrum can be analysed into a progression of the excited state frequencies 282, 584, 726, 965 and 1261 cm^{-1}. With the solidification of the liquid and lowering of temperature to $-180°C$, the 0, 0 band does not show any further appreciable shift. It is thus evident that the major shift in the position of the 0, 0 band occurs when the change of vapour to liquid state takes place.

Similar disappearance of bands due to $n \rightarrow \pi^*$ transition in the liquid and solid states was observed in the case of pyridine and the isomeric picolines (Banerjee, 1956 and 1957). This was explained by assuming that in the condensed phases, the molecules of these compounds form associated groups through the nitrogen non-bonding electron and hydrogen atom of the neighbouring molecules. The results observed in the case of 3-bromopyridine also seem to corroborate the view mentioned above and indicate a similar association of molecules in the liquid and solid states.

It can be seen from Table II that a single excited state frequency 970 cm^{-1} occurs in the case of the liquid and 965 cm^{-1} in the case of the solid state in place of two such frequencies 946 cm^{-1} and 1016 cm^{-1} observed in the spectrum due to the vapour. This is evidently due to broadening of the bands in the former cases caused by the intermolecular field and to consequent overlapping which gives a mean frequency.

2-bromopyridine

(*a*) *Spectrum in the vapour phase*

The spectrum due to the 2-bromopyridine in the vapour state yields only one system of discrete bands in the region 37000 cm^{-1} to 39000 cm^{-1}, as can be seen from Figs. 4a and 4b. With the increase in the length of the absorbing path and in the pressure of the absorbing vapour, unlike in the case of 3-bromo isomer, no sharp, narrow and line-like bands due to $n \rightarrow \pi^*$ transition were observed in this case. The weak continuous absorption extending up to about 900 cm^{-1} on the long wavelength side of the 0, 0 band due to the $\pi \rightarrow \pi^*$ transition at higher temperature and pressure observed in this case may be due to $v \rightarrow 0$ transition coupled to the electronic transition in $\pi \rightarrow \pi^*$ system. Thus the $n \rightarrow \pi^*$ system is absent in this case. These results thus agree with those reported by Stephenson (1954).

(i) $\pi \rightarrow \pi^*$ transition (Transition II)

The strong band at 36958 cm^{-1} has been taken to be the 0,0 band and the analysis of the other bands has yielded the excited state vibrational frequencies 136, 280, 653, 742, 954, 1053 and 1554 cm^{-1} as shown in Table III.

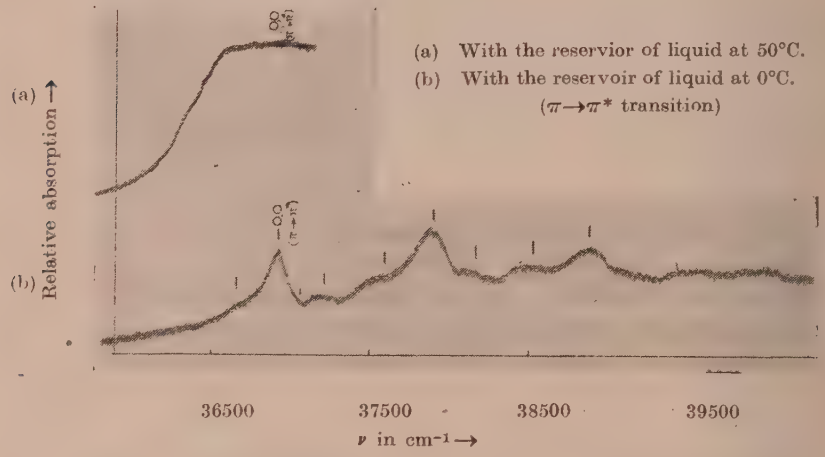

Fig. 4. Microphotometric records of ultraviolet absorption spectra of 2-bromopyridine in the vapour state.

The infrared absorption spectra of a very thin film of 2-bromopyridine was studied with rocksalt optics in order to find out the ground state vibrational frequencies. The wave numbers of the observed infrared bands are 698 (ms), 756 (s), 988(ms), 1040(w), 1075(s), 1103(s), 1148(vw), 1282(vw), 1418(s), 1451(ms) and 1563(s), the strengths of absorption being given in the parentheses.

The upper state vibrational frequencies 653, 742 and 954 cm^{-1} can be co-related to the ground state frequencies 698, 756 and 988 cm^{-1} observed in the infrared absorption. The vibrational frequencies 1053 cm^{-1} and 1554 cm^{-1} in the excited state probably correspond to the infrared frequencies 1075 cm^{-1} and 1563 cm^{-1} respectively.

As regards the band at a distance of 280 cm^{-1} on the shorter wavelength side of the 0, 0 band, a band at 292 cm^{-1} on the longer wavelength side has been recorded. This band which probably represents the ground state frequency has not been observed in the infrared absorption because of limitation of NaCl optics used. The band at 136 cm^{-1} on the shorter wavelength side of the 0, 0 band might represent a $0 \rightarrow v'$ transition. The assignment is not improbable for such low frequency transition is observed in the case of 3-bromo isomer and other substituted pyridine compounds (Rush and Sponer, 1952).

TABLE III

Ultraviolet absorption bands of 2-bromopyridine in the vapour state

Wave No. (cm^{-1}) and intensity	Assignment	Wave No. (cm^{-1}) and intensity	Assignment
Transition I		Transition II	
		36666 (w)	0−292
		36958 (s)	0, 0
		37094 (w)	0+136
Absent		37238 (m)	0+280
		37611 (m)	0+653
		37700 (w)	0+742
		37912 (s)	0+954
		38011 (vw)	0+1053
		38178 (m)	0+1220
			0+280+954
		38512 (ms)	0+1554
		38870 (s)	0+2×954

A comparison of the absorption spectra of 2-bromopyridine and pyridine in the vapour state shows that the 0,0 band of 2-bromopyridine is shifted by about 1392 cm^{-1} towards red with respect to that of the latter compound. A similar substitution by CH_3 group in α-picoline shifts the 0, 0 band only by 730 cm^{-1}.

(*b*) *Spectra of solutions*

When 2-bromopyridine is dissolved in alcohol, at a concentration of .01% by weight and a path length of 5 mm, the band system due to $\pi \rightarrow \pi^*$ transition appears with the 0, 0 band at 36753 cm^{-1} and the other bands are represented by progression of frequencies 971 cm^{-1} and 655 cm^{-1} in the excited state (Fig. 5c). It can be seen that in the case of .01% solution in alcohol the 0,0 band is shifted by about 200 cm^{-1} towards long wavelengths from the 0,0 band due to the vapour.

On gradually increasing the concentration of the solution from .01% to .08% by weight, a continuous absorption due to $v \rightarrow 0$ transition of $\pi \rightarrow \pi^*$ system is observed in the region 35500 cm^{-1} to 36700 cm^{-1} as is evident from the absorption curve reproduced in Fig. 5. A similar absorption is also observed in case of .08% solution in 3-methyl pentane, but no band system due to $n \rightarrow \pi^*$ transition as observed in the case of 3-bromopyridine could be detected in this case.

This is an agreement with the conclusions of Stephenson (1954) who earlier studied the absorption spectra of solution of 2-bromopyridine in alcohol and in iso-octane and from the similarity of the two absorption curves concluded that the $n \rightarrow \pi^*$ transition is absent in the spectrum due to the 2-bromopyridine molecule.

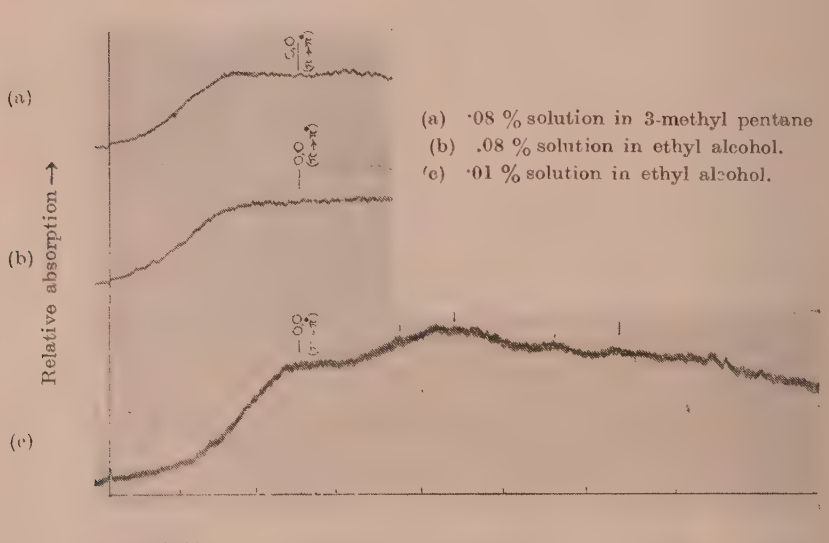

Fig. 5. Microphotometric records of the ultraviolet absorption spectra of solutions of 2-bromopyridine.

(c) *Spectrum in the liquid and solid states*

In the spectrum of 2-bromopyridine in the liquid state only one system of discrete bands consisting of three broad bands due to Transition II is observed (Fig. 6), the band at 36571 cm^{-1} being taken as the 0,0 band of this system. Thus the 0, 0 band shifts by about 387 cm^{-1} towards longer wavelengths with liquefaction of the vapour. The other bands can be assigned to a progression of the excited state frequency 918 cm^{-1}. When the liquid is frozen and cooled to about −180°C, these bands become a little sharper, but the bands are not resolved into sharper components. The shift of the bands with liquefaction of the vapour is much larger than that observed in spectrum due to the solution in alcohol. The 0,0 band in this case is at 36479 cm^{-1} and the other two bands are assigned to a progression of the upper state vibrational frequency 971 cm^{-1}. Thus with

solidification and cooling the substance to about 180 C. the 0,0 band undergoes a small shift of 92 cm^{-1} towards red.

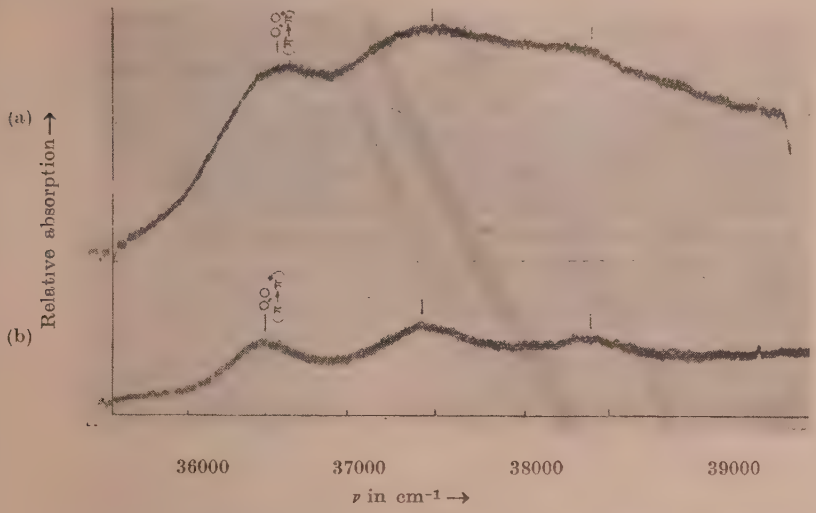

Fig. 6. Microphotometric records of the ultraviolet absorption spectra of 2-bromopyridine.
(a) Liquid at 32°C.
(b) Solid at –180°C.

TABLE IV

Ultraviolet absorprtion bands of 2-bromopyridine

	Liquid at 32°C		Solid at –180°C		Solution at 32°C			
	Wave No. (cm^{-1}) and intensity	Assignment	Wage No. (cm^{-1}) and intesnity	Assignment	Wave No. (cm^{-1}) and intensity	Assignment	Wave No. (cm^{-1}) and intensity	Assignment
Transition I					.08% sol. in alcohol		.08% sol. in 3-methyl pentane	
	Absent		Absent		Absent		Absent	
Transition II					.01% sol. in alcohol			
	36571 (s)	0, 0	36479 (s)	0, 0	36753 (s)	0, 0		
					37408 (m)	0+655		
	37489 (vs)	0+918	37450 (s)	0+971	37724 (s)	0+971		
					38379 (s)	0+971+655		
	38406 (ms)	0+2×918	38420 (ms)	0+2×971	38697 (s)	0+2×971		

When thicker film of thickness of the order of 10 microns is used, the $\pi \rightarrow \pi^*$ system produces continuous total absorption but no other band system in the low energy region corresponding to $n \rightarrow \pi^*$ transition is produced by the substance either in the liquid state or in the solid state at $-180°C$.

It is concluded that in the case of 2-bromopyridine the $n \rightarrow \pi^*$ transition is absent whether the substance is in the vapour phase, in solutions or in the states of aggregation. As postulated by Stephenson (1954) this may be due to the inductive attraction of the halogen atom attached to the carbon atom adjacent to the nitrogen atom which increases the binding energy of the non-bonding electron over that existing in pyridine, thereby shifting the $n \rightarrow \pi^*$ transition into the spectral region of $\pi \rightarrow \pi^*$ transition and the situation is not altered when the molecules are in solutions and also in the state of aggregation.

ACKNOWLEDGMENT

The author is indebted to Professor S. C. Sirkar, D.Sc., F.N.I., for his kind interest and guidance in the work.

REFERENCES

Banerjee, S. B., 1956, *Ind. J. Phys.*, **30**, 480.
„ 1957, *Ibid.*, **31**, 11.
Kasha, M., 1950, Discussion of the Faraday Society, No. **9**, 14.
Misra, T. N., 1959, *Ind. J. Phys.*, **33**, 276.
Roy, S. B., 1958, *Ind. J. Phys.*, **32**, 323.
Rush, J. H. and Sponer, H., 1952, *J.Chem. Phys.*, **20**, 1847.
Sirkar, S. C. and Misra, T. N., 1959, *Ind. J. Phys.*, **33**, 45.
Stephenson, H. P., 1954, *J. Chem., Phys.*, **22**, 1077.

Letters to the Editor

The Board of Editors will not hold itself responsible for opinions expressed in the letters published in this section. The notes containing reports of new work communicated for this section should not contain many figures and should not exceed 500 words in length. The contributions must reach the Assistant Editor not later than the 15th of the second month preceding that of the issue in which the letter is to appear. No proof will be sent to the authors.

12

ON THERMAL CONDUCTIVITY OF ALUMINIUM AT LOW TEMPERATURES

H. N. PATIL

GUJARAT COLLEGE, AHMEDABAD

(*Received, June* 25, 1960)

There are two mechanisms conducting the heat in a metal. As in non-conductors there is transfer of heat by the lattice waves and in addition a transfer by the electrons. The total heat conductivity is thus made up of two components: K_g the lattice conduction, and K_e the electronic conduction. The electronic heat resistance $W(=1/K_e)$ can be written as $W = W_0 + W_i$, where W_0 is the resistance due to impurity scattering and W_i is the resistance due to the scattering of the conduction electrons by the lattice waves and imperfections. W_0 is of the form β/T, and W_i, at temperatures below about $\theta/10$, is of the form αT^2.

Thus neglecting the lattice conduction K_g in the case of pure metals, we have for total thermal resistance $W = \alpha T^2 + \beta/T$. A plot of WT against T^3 over a certain range of temperature should be a straight line with a slope α.

In case of experimental curve for Al drawn by Andrews and his coworkers (1951), it is seen that such plot has two linear sections instead of one having slopes $\alpha = 2.470 \times 10^{-5}$ cm. Watt.$^{-1}$ °K^{-1} for the range of temperature 3.5°K to 12.5°K, and $\alpha = 6.00 \times 10^{-5}$ cm Watt^{-1} °K^{-1} for the range 2 to 4°K.

This observed variation in slope is explained on how θ the Debye characteristic temperature changes with T. Rosenberg (1957) and others have observed such variations in slope in case of Cd, Zn and Hg, etc.

Semi-analytic method has been used in the case of Al to study the temperature dependence of θ at low temperatures (Seitz and Trunbull, 1956). The values of θ in the region where it first departs from θ_0, and the value of θ at 0°K, are given

by $\theta^3 = \theta_0^3[1-f'(s, t)\,(T/\theta_0)^2]$. The parameters s and t are determined from the values of elastic constants at 0°K and values of f' for *bcc* and *fcc* lattices are determined from tables (Seitz and Turnbull, 1956). Using the elastic constants at 0°K for Al, $c_{11} = 1.226$, $c_{12} = 0.708$, $c_{44} = 0.306$, the characteristic temperature, in case of central forces plus electron gas model is given by $\theta = 426.6-0.0544\,T^2$.

From this expression, it is seen that the temperature region in which θ starts changing with temperature approximately corresponds to the region in which the value of slope, α changes. But from the ratio of values of α it seems necessary, in addition to the study of variation in θ, to consider lattice conductivity because of impurities in the specimen and scattering by boundaries, the dominant source of thermal resistance at very low temperature. The lattice component would cause the curve WT against T^3 to dip below (Handbuch der Physik XIV p. 247).

Author's thanks are due to Principal Y. G. Naik for useful discussions.

REFERENCES

Andrews, F. A. Webber, R. T. and Spohr, D. A. 1951, *Physical Review*, **84**, 994.
Dekker, A. J. 1957, *Solid State Physics*, p. 295.
Rosenberg, H. M. 1957, *Phil. Mag*, **2**, 541.
Seitz and Turnbull, 1956, *Solid State Physics*, Vol. 2, p. 285.

IMPORTANT PUBLICATIONS

The following special publications of the Indian Association for the Cultivation of Science, Jadavpur, Calcutta, are available at the prices shown against each of them:—

TITLE	AUTHOR	PRICE
Magnetism ... Report of the Symposium on Magnetism		Rs. 7 0 0
Iron Ores of India	... Dr. M. S. Krishnan	5 0 0
Earthquakes in the Himalayan Region	... Dr. S. K. Banerji	3 0 0
Methods in Scientific Research	.. Sir E. J. Russell	0 6 0
The Origin of the Planets	.. Sir James H. Jeans	0 6 0
Active Nitrogen— A New Theory.	.. Prof. S. K. Mitra	2 8 0
Theory of Valency and the Structure of Chemical Compounds.	.. Prof. P. Ray	3 0 0
Petroleum Resources of India	.. D. N. Wadia	2 8 0
The Role of the Electrical Double-layer in the Electro-Chemistry of Colloids.	.. J. N. Mukherjee	1 12 0
The Earth's Magnetism and its Changes	.. Prof. S. Chapman	1 0 0
Distribution of Anthocyanins	.. Robert Robinson	1 4 0
Lapinone, A New Antimalarial	.. Louis F. Fieser	1 0 0
Catalysts in Polymerization Reactions	.. H. Mark	1 8 0
Constitutional Problems Concerning Vat Dyes.	.. Dr. K. Venkataraman	1 0 0
Non-Aqueous Titration	.. Santi R. Palit, Mihir Nath Das and G. R. Somayajulu	3 0 0
Garnets and their Role in Nature	.. Sir Lewis L. Fermor	2 8 0

A discount of 25% is allowed to Booksellers and Agents.

NOTICE

No claims will be allowed for copies of journal lost in the mail or otherwise unless such claims are received within 4 months of the date of issue.

CONTENTS

Indian Journal of Physics Vol. 34, No. 8 August, 1960

PAGE

39. Nuclear Spin Echoes and Molecular Self-Diffusion in Liquids— S. K. Ghosh and S. K. Sinha 339

40. Absorption of Microwaves in Cyclohexanol and Cyclopentanol and their Solutions— T. J. Bhattacharyya 358

41. Light Absorption in Paramagnetic Ions in State of Solution. Part II—Ni^{++} ion— A. Mookherji and N. S. Chhonkar 363

42. On the Electronic Spectra of 2-Bromo and 3-Bromopyridine in Different States and in Solutions— T. N. Misra 381

LETTER TO THE EDITOR :

12. On Thermal Conductivity of Aluminium at Low Temperatures— H. N. Patil 395

PRINTED BY KALIPADA MUKHERJEE, EKA PRESS, 204/1, B. T. ROAD, CALCUTTA-35
PUBLISHED BY THE REGISTRAR, INDIAN ASSOCIATION FOR THE CULTIVATION OF SCIENCE
2 & 3, LADY WILLINGDON ROAD, CALCUTTA-32